AN ALTERNATIVE TO THE CLASSICAL SPECIFICATION OF BOUNDARY CONDITIONS IN FINITE ELEMENT STRESS ANALYSIS

by Christopher John Brown

Submitted to the University of Cape Town in fulfillment of the requirements for the degree of Master of Science in Engineering.

September 1977

ABSTRACT

A development of the displacement method of finite element analysis is presented which serves to effectively bypass conventional boundary condition specifications. Indeterminate equations pertaining to boundary degrees of freedom are replaced in the assembly matrix by an alternative form of equation based on the strain/displacement relationship of finite elements. The computer programming of the proposed method is described, and a series of proving runs made on typical mesh configurations is discussed.

ACKNOWLEDGEMENTS

To Mr. J. E. Newmarch who, as project supervisor, provided invaluable aid and advice, especially in the field of computer usage and programming.

To Mr. H. Scheffel, head of the Development of Rolling Stock section of the South African Railways, for providing the topic of this thesis and for his support in enabling it to be accomplished.

To Professor R. K. Dutkiewicz under whose jurisdiction the project was executed.

To the workshop staff of the University of Cape Town for the preparation of the experimental models.

To the General Manager of the South African Railways for the permission and financial support required to undertake the project.

To my wife, Anja, for the typing of the report.

CONTENTS

Appendix B ......

NOMENCLATURE

[B]	matrix containing derivatives of [N]
[D]	matrix of elastic-strength properties
f	photoelastic fringe value
{f}	element nodal force matrix
{F}	continuum nodal force matrix
F_q	force at node q
GJR	computer packaged Gauss-Jordan matrix solution programme
[J]	Jacobian matrix
[K]	assembled continuum stiffness matrix
[K′]	element stiffness matrix (also $[k_e]$)
K_{qr}	coeffecient of [K]
[N]	matrix of shape functions
Q(x)	the quadratic form of the linear system Ax=b
u_i, v_i	Cartesian components of the displacement of node i
x,y,z	Cartesian or global coordinates
$\{\delta\}$	continuum nodal displacement matrix
$\{\delta\}^e$	element nodal displacement matrix
δ_r	displacement of node r
$\{\varepsilon\}$	strain matrix
π_c	potential energy of the continuum
π_e	potential energy of an element
$\{\sigma\}$	stress matrix
ξ, η, ζ	local coordinates
$A \subset B$	A is a subset of B
$\Longrightarrow$	implies

finite element method, capable of analysing the local stress field surrounding a stress-raiser in a two- or three-dimensional body; the technique being easy to use, accurate and economical in terms of computer usage and analysis time.

The attainment of this objective can be split into three parts, namely:

1) the formulation of the required theory;
2) the development and construction of the computer programmes;
3) the experimental testing and verification of the technique.

These sections, although categorically distinct, have been closely inter-related during development. For the purpose of clarity however they are presented separately in this report.

1.3 THE BACKGROUND TO THE PROJECT

Recourse to literature available in the field of finite element work has played a fundamental rôle in three phases of the project:

1) the choice of the type of finite element method to be used;
2) the construction of a theoretical basis for the development of the model;
3) the construction of the practical computational basis for the technique devised.

A survey of the literature used can thus be divided into these categories. However only the first, the choice of a finite element method, is presented at this juncture. The treatment of the other two categories is embodied within the text of the relevant sections of the report.

The search for a suitable method has been made as broad as possible, being aimed at either unearthing an existing technique capable of satisfying the objective or, failing this, to enable the sound choice of a method which is readily convertible to do so.

In the analysis of deformable bodies there are two basic methods of mathematically formulating a problem: either through the use of

differential equations/3.........

boundaries and an assumed equilibrating stress field in each element, and is based on a modified complementary energy principle. The mixed method is derived from Reissner's variational principle and is based on an assumed displacement field which is continuous over the entire solid, and on assumed stress fields for individual elements. Finally there exists a group of methods based on various other variational principles.[7,8] However, none of the above models and methods escape the boundary specification criterion. Any advantages of the equilibrium model and the hybrid and mixed methods in terms of control over the specification of stresses are offset by the paucity of literature relating to the practical implementation of these models.

Thus in the absence of a method capable of the direct solution of the problem of indeterminate boundary conditions it appears that the compatible model in the form of the displacement method, as the most widely used[9] and best documented method of finite element analysis, provides the best choice of a basis on which to develop the technique required.

CHAPTER 2

THE THEORY OF THE PROPOSED METHOD

2.1 INTRODUCTION

The chapter is concerned with the theory of a procedure based on the displacement method of finite element analysis and capable of circumventing the specification of standard boundary conditions. The first section deals with the constraints imposed by the objectives of the project and the explicit formulation of the method in the light of these. The second section is concerned with the theoretical assessment of various aspects of the proposed method.

A summary of the standard displacement method as developed in its explicit form is contained in Appendix A.

2.2 THE FORMULATION OF THE METHOD

The development of the theory for a method which provides a solution within the project constraints is presented in the section.

2.21 Constraints Imposed on the Method

2.211 Defining the class of problems to be dealt with. For practical purposes it is necessary to restrict the field of solid mechanics problems to which attention is given in this project. There are three classes of problems determined by the stress-strain relationship and the strain-displacement relationship, [1] namely:

1) linear: in which both of the above relationships are assumed linear;
2) non-linear stress-strain relationship: including non-linear material problems, plasticity, creep and non-linear field problems;
3) non-linear strain-displacement relationship: including geometrically non-linear problems, large displacements, and structural instability.

Although the concept developed in this project most probably applies to all of these classes, the thesis confines itself to the first

class,/6.........

class, as it is the logical starting point.

The constraints applied to the linear class of problems can be summarised as: [1,3]

1) small strains;
2) small displacements;
3) linear elastic relationships as given by $\{\sigma\} = [D]\{\varepsilon\}$;
4) linear strain-displacement relationships as given by $\{\varepsilon\} = [B]\{\delta\}^e$;
5) assembly equations of the general form $[K]\{\delta\} = \{F\}$;
6) continuity of displacements throughout the mesh;
7) approximate satisfaction of the conditions of equilibrium.

The method is thus developed for the analysis of elastic, homogeneous and isotropic materials with small strains and displacements.

2.212 The restrictions on the loading data. With reference to equations (xii) and (xiii) of Appendix A it can be seen that the assembly equations

$$\{F\} = [K]\{\delta\}$$

comprise a set of force/displacement equations of the form

$$F_q = K_{q1}\delta_1 + K_{q2}\delta_2 + \ldots\ldots\ldots + K_{qr}\delta_r .$$

Each equation relates a force component at a node to the displacements of all nodes assosciated with it, by means of the stiffness constants, K , which are functions of nodal coordinates and elasticity constants (Appendix A equations (ix) and (x)). In conventional displacement method analysis, forces are specified as constraints to be applied to the assembly equations prior to solution; the forces at internal nodes being set to zero by virtue of their state of equilibrium, and either the forces or the displacements being specified at the boundary nodes. It is evident that the analysis of a mesh whose boundary nodes are internal to the physical boundaries of the relevant component is complicated by the difficulty of specifying the forces acting on these nodes, and a means of bypassing this specification must thus be determined.

In the/7.........

In the displacement method, the assembly equations

$$[K]\{\delta\} = \{F\}$$

comprise a set of equations having an infinite number of solutions prior to the specification of displacement constraints. This arises from the rigid-body motions inherent in these equations. The stipulation therefore exists to specify a minimum number of specifically orientated displacements, equal to the possible types of rigid-body motions, in order to locate the body in space.[1,6,10] These displacement constraints are conventionally applied at the boundary nodes of the mesh.

The objective of the project is to develop an alternative loading specification system which makes use of experimentally obtained data. However, forces and displacements cannot be directly measured at points on the interior of a body - the commonly used experimental methods provide a direct measure of surface strain.

It is therefore required that the method developed be capable of utilising input data in the form of strains. The exclusive use of such data presupposes the fact that no conventional loading information is available.

The consideration of the case of a localised region of interest in a three-dimensional body, eg. a corner, imposes a severe constraint on the method: the boundary surfaces of the mesh which lie in the interior of the body are obviously inaccessible for the purpose of experimentally determining data at these nodes. The method must thus provide a means whereby the specification of loading conditions on the accessible surfaces suffices to define the loading field over the entire mesh.

2.22 The Proposed Form of the Loading Data

Intuitively it appears that experimentally determined strains could be used to supply input data in the following possible ways:

1) convert the strains to stresses and hence to forces;

2) convert the strains to nodal displacements and input as boundary conditions;
3) substitute the numerical values of the strains directly into an intermediate stage of the finite element method formulation.

These proposals are briefly examined in turn:

1) Strains are readily convertible to stresses by means of Hooke's Law [3], and thus strains measured at the boundary nodes of a local mesh could supply the stress values at these points. In the two-dimensional case it is possible to average these stresses across the boundary and to estimate the statically equivalent nodal forces from them, as described by Zienkiewicz [1]. The extension of this method to the three-dimensional case cannot meet the requirements of the constraint given in section 2.212, as the strains at nodes internal to the body cannot be experimentally measured.
2) Strains measured at a point can give no indication as to the displacement of that point relative to the surrounding body [3]. A strain measured within an element provides a measure of the relative displacement of the nodes with respect to one another, but cannot supply the absolute values of these displacements due to the possibility of rigid-body motion. For example, in the case of a two-dimensional triangular element, three strain components can be measured whereas six degrees of freedom exist within the element. Furthermore, as in the case of proposal 1, the approach cannot meet the requirements for three-dimensional work.
3) This proposal can be viewed in two ways. In the first, the substitution of strain values into an intermediate step in the displacement method, such as into equations (viii) and thence (ix) of Appendix A, is of no consequence as the relevant forces and displacements remain unspecified. The second option is to construct a relationship between the strain values and the variables of the assembly equations, ie. the displacements, and to input this information

into the assembly set prior to solving for the displacements. This relationship will not be of the same form as the force - displacement equation, and it is possible that the conventional restrictions might be relaxed, thereby permitting the three - dimensional solutions sought.

It is evident that the third proposal, that of constructing strain-displacement equations, provides the most suitable means whereby a method may be formulated.

Having specified that the method is to incorporate strain-displacement "loading equations" into the set of assembly equations, it now remains to determine the form of these equations and the manner in which they are to be incorporated.

It is proposed, at this stage of the formulation of the theory, that the strains be measured at convenient locations on the body, each of these points being precisely related to the finite element mesh. Let each measured point represent the centroid of an element in the two - dimensional case, and the centroid of an element face in a three - dimensional analysis.

Every measured strain can be related to the relative displacements of the nodes of its element by the relationship

$$\{\varepsilon\} = [B]\{\delta\}^e$$

(cf. equation (vi) of Appendix A). It is immediatly evident that this formulation ensures that the order of the displacement polynomial and the type of shape function (equations (i) and (iv)) correspond to those incorporated in the assembly matrix to be adapted. Furthermore, the displacements are global displacements and are thus entirely compatable with those occuring in the conventional force-displacement equations. The above relationship provides a set of three linearly independent equations per element, whereby each of the components of measured surface strain is uniquely related to the nodal displacements.

The strain - displacement equations can be used in one of two ways.

1) The/10.........

1) The three equations relating the strain components to the nodal displacements can be algebraically summed per element, thereby obtaining an averaged form of the experimental data measured at the point in question.
2) The equations can be used individually. Thus three equations can be generated by one complete strain measurement (eg. a strain rosette), and the method requires one third of the quantity of experimental data needed for method 1.

The discussion of the relative merits of the two methods is left to the experimental section of the report.

2.23 The Statement of the Method

As described in section 2.212, conventional analysis requires the specification of the forces on the boundary nodes of the mesh, a stipulation which cannot readily be met for localised meshes. The method proposed is to bypass this limitation by removing from the assembly set all the force - displacement equations requiring such specification. The remaining set of equations is thus singular, having a rank less than the number of unknowns. Supplementing this set with a number of strain - displacement equations equal to the number of force - displacement equations removed could restore the rank to the level required for non - singularity, and a unique solution of the displacements would thus be obtainable.

The proposed method can be seen to bypass the explicit specification of boundary nodal forces, but it does not circumvent the necessity for constraining certain displacements (described in section 2.212). This aspect is dealt with more fully in the next section.

The steps incorporated in the method can thus be summarised as:

1) construct a mesh local to the region of interest;
2) note all the boundary nodal degrees of freedom which cannot be specified, ie. where the conventional force - displacement

loading conditions are not known;

3) measure strains at the centroids of chosen elements, obtaining sufficient data for use in the replacement of the boundary force - displacement equations;
4) perform the conventional finite element analysis up to and including the assembly of the general stiffness matrix;
5) utilise the elemental strain - displacement relationships to obtain the relevant strain - displacement equations;
6) remove the relevant boundary force - displacement equations and append an equal number of strain - displacement equations to the assembly matrix;
7) proceed in the conventional manner with the solution of the assembly matrix for displacements, and the derivation of the stress and strain fields.

It should be noted that the method is described above in the form in which it was originally construed. Subsequent work has indicated that this model tends to be simplistic and certain qualifications must be made to safeguard the accuracy of the solution. This work is covered in sections 2.3, 4.4 and 4.5.

2.3 A CONSIDERATION OF THEORETICAL ASPECTS OF THE PROPOSED MODEL

In the previous section, the evaluation of the proposal was described in terms of satisfying the objective set for the method. The validity of the proposed method in terms of its underlying theory remains to be examined, and various theoretical aspects of this question are dealt with in this section.

Some of the points covered here were not evident in the initial studies of the method, and their significance only became apparent when the experimental tests were made.

2.31 The Effect on the Principles of the Minimisation of Potential Energy

In order to examine the validity of the proposed method in terms of the basic theory of the displacement method, it is necessary to study the effects, if any, made on the principles of energy minimisation upon which the finite element method rests.

The treatment of variational theory is provided in many publications (see, for instance, references 1, 4-6, 8, 11-15), but a summary is provided here for the sake of clarity.

The potential energy can be formulated for each element e as

$$\pi_e = \frac{1}{2}\int_{ve} \{\sigma\}^T \{\varepsilon\} \, dv - \{\delta\}_e^T \{f\}$$

With strains and stresses expressed as

$$\{\varepsilon\} = [B]\{\delta\}_e \quad \text{and} \quad \{\sigma\} = [D][B]\{\delta\}_e$$

(Appendix A (vi) and (viii))

this becomes, per element

$$\pi_e = \frac{1}{2}\{\delta\}_e^T \int_{ve} [B]^T [D][B] \, dV \{\delta\}_e - \{\delta\}_e^T \{f\}$$

$$= \frac{1}{2}\{\delta\}_e^T [k_e] \{\delta\}_e - \{\delta\}_e^T \{f\} .$$

The potential energy of the continuum is then formed by joining the elements in the appropriate manner, which results in

$$\pi_c = \frac{1}{2}\{\delta\}^T [K] \{\delta\} - \{\delta\}^T \{F\}$$

At this stage both the element stiffness matrix $[k]$ and the assembly stiffness matrix $[K]$ are positive semi - definite.[1,6,16] This arises from the fact that the set of rigid - body displacements is included in the displacement functions, and since rigid states are synonymous with solutions of the homogeneous or inextensional set of equations, the necessary conditions for positive definiteness of the matrices ($\{\delta\}^T [K] \{\delta\} > 0$ for all $\{\delta\} \neq 0$) are not met. The attainment of an absolute minimum of potential energy by differentiating the potential energy functional with respect to the nodal displacements cannot be realised prior to the alteration within the functional of the stiffness matrix to the positive definite form [16]. This is achieved by prescribing a minimum number of displacements, equal to the number of rigid - body degrees of freedom of the body, and partitioning the assembly stiffness matrix accordingly, ie.

$$\pi_c = \frac{1}{2}\left\{\delta_1^T \;\; \delta_2^T\right\} \begin{bmatrix} K_{11} & K_{12} \\ K_{12} & K_{22} \end{bmatrix} \begin{Bmatrix} \delta_1 \\ \delta_2 \end{Bmatrix} - \left\{\delta_1 \;\; \delta_2\right\} \begin{Bmatrix} F_1 \\ F_2 \end{Bmatrix}$$

where displacements $\{\delta_1\}$ are unknown and $\{\delta_2\}$ are prescribed, and forces $\{F_1\}$ are presented or are to be presented, and $\{F_2\}$ are unknown. The sub - matrix $[K_{11}]$ is positive - definite and rank sufficient by virtue of this formulation. The subsequent application of the minimising principle

$$\frac{\partial \pi_c}{\partial\{\delta\}} = 0$$

(alternatively described as $\Delta \pi_c = 0$), results in

$$[K_{11}]\{\delta_1\} = \{F_1\}$$

Thus if only the minimum number of displacements is prescribed, the above set of equations describes the homogeneous system having the unique solution $\{\delta\} = 0$ for $\{F\} = 0$. A subsequent specification of loading constraints (which conventionally are in the form of forces and/or displacements) to these equations will result in a unique solution of the then nonhomongeneous system.

The proposed method, deviates from convention in that loading constraints are applied by means of equations which are included into the assembly matrix. However, it is evident from the above paragraphs that provided the minimum number of displacements is prescribed to ensure the positive difiniteness of the assembly matrix, any loading constraints applied to the subsequently formulated set of force-displacement equations are divorced from consideration of the minimisation of potential energy.

2.32 The Rank/14..........

2.32 The Rank Sufficiency of the Proposed Set of Equations

In the previous section it was shown that the proposed adaption of the set of assembly equations occurs after the minimisation procedures have been executed, and is therefore equivalent in this respect to the conventional loading method. However, it remains to be shown that the adapted set of equations is capable of constituting a nonhomogeneous system having a unique solution.

The linear algebra theory incorporated in the following discussion is drawn from Noble[16] and Nering[46], and the reader is referred to these texts for definitions and descriptions of the concepts involved.

The set of equations under consideration can be expressed in the general form as

$$\sum_{j=1}^{n} K_{ij} \delta_j = F_i \quad \ldots\ldots \quad i = 1, \ldots, n$$

or in matrix form as

$$[K]\{\delta\} = \{F\}$$

A unique solution for the displacements $\{\delta\}$ can be obtained if and only if the rank of the augmented matrix $[K,F]$ is equal to that of matrix $[K]$, this in turn being equal to the number of unknown variables in $\{\delta\}$. The term rank can be defined in various ways, all of them having the same value:

i) the dimension of the column or row space of a matrix;
ii) the maximum number of linearly independent columns or rows of matrix;
iii) the number of rows or columns in row - echelon form;
iv) the order of the largest nonsingular submatrix;
v) the order of the largest non-zero determinant.

For the case in hand, the rank can thus be interpreted as the number of linearly independent equations in the set.

The previously discussed specification of a minimum number of

displacements/15.........

posed matrix $[K]^T$ of the homogeneous system be labelled

$$L_1 , L_2 , L_3 , \ldots\ldots , L_i , \ldots\ldots\ldots\ldots , L_n$$

where L_i is the i th column of $[K]^T$. The set of vectors can be described as spanning the space of dimension n. Since a strain - displacement equation contains the same displacement variables as the force - displacement equations, its vector representation exists in the same vector space. Let S_1 be any relevant strain - displacement vector (ie. the coefficients of an equation) and write the vector in column form. In a manner similar to that in which Steinitzs' Replacement Theorem is formulated [16], consider the set of vectors obtained by adding the vector S_1 to the set of L's

$$S_1 , L_1 , L_2 , \ldots\ldots\ldots , L_i , \ldots\ldots , L_n$$

Since the L's span the vector space, S_1 can be expressed as a linear combination of the L's. Hence, by the theorem that a set of nonzero vectors $u_1 , \ldots , u_q$ is linearly dependent if and only if one of the u_k, for some k, is a linear combination of the preceding $u_1 , \ldots , u_{k-1}$, the above set is linearly dependent and one of the vectors can be expressed as a linear combination of the preceding vectors. By relabelling the L's if necessary, arrange that this vector is L_n. The vector space can thus be spanned by the set obtained by omitting L_n, ie. by the set

$$S_1 , L_1 , L_2 , \ldots\ldots , L_{n-1}$$

Let S_2 be another relevant strain - displacement vector. Add this vector in front of the new set

$$S_2 , S_1, L_1, L_2, \ldots\ldots\ldots , L_{n-1}$$

As before, S_2 can be expressed as a linear combination of the remaining vectors, ie. one of the vectors can be expressed as a linear combination of the preceding. Since S_2 and S_1 are independent, this means that one of the L's can be expressed as a linear combination of the preceding vectors. By relabelling if necessary, it can be arranged that this vector is L_{n-1}. The vector space is thus spanned by omitting this

vector,/17.........

vector, ie. by the set

$$S_2, S_1, L_1, L_2, \ldots\ldots\ldots, L_{n-2}$$

This procedure can be repeated as many times as there are strain equations. However, it differs from the method proposed in this thesis in that it involves the choice of a suitable L_i to be substituted for by a given S_j, whereas the method requires the choice of a suitable strain - displacement equation (S_j) to be substituted for a given force - displacement equation pertaining to a boundary node (L_i).

Should a strain - displacement equation be substituted for a force-displacement equation which does not belong to its linearly dependent subset, and all the other substitutions be correctly performed into their relevant linearly dependent subsets, then that equation would remain linearly dependent on its subset. The entire set of equations would thus be linearly dependent and the matrix $[K]$ vectors would span a space of dimension n-1, ie. the matrix would be singular and an infinity of solutions possible.

Should two or more substitutions of strain - displacement equations be misplaced it is possible that a cross - cancellation of linear dependence relationships could occur; eg. if S_1 is linearly dependent on vectors L_2, L_3, L_4, L_5 and is substituted for L_{10}, and S_2 is linearly dependent on vectors L_7, L_8, L_9, L_{10} and is substituted for L_3, then the system of vectors is linearly independent and identical to that which would have been obtained had the substitutions been performed in the correct manner.

It is thus evident that a random choice, without examining the linear dependence relationships, of the strain - displacement equations for substitution will result in an uncertainty with regards to the solution: the set of equations will be rank-sufficient if and only if no linearly dependent subsets have been created.

In practice,/18.........

In practice, the best way to ensure the linear independence of the adapted set of equation is to utilise, at the substitution stage, the approach described in the preceding discussion. This can be listed in step form as follows:

1. transpose the conventional homogeneous assembly matrix $[K]$ to form $[K]^T$ (in effect no change occurs since $[K]$ is symmetric);
2. transpose the vector representations (ie. the coefficients) of all the strain - displacement equations, to form $[R]^T$;
3. augment these vectors to $[K]^T$ to form $\left[[K]^T \mid [R]^T\right]$;
4. identify the boundary force - displacement equation to be replaced and locate its representative column in $\left[[K]^T \mid [R]^T\right]$;
5. reduce $\left[[K]^T \mid [R]^T\right]$ to the row - echelon form $\left[[I] \mid [R']\right]$;
6. determine which of the columns, if any, of $[R']$ are linearly dependent on the relevant column of $[I]$: if there is none, no substitutions can possibly be made; if there is more than one, choose the most convenient of the relevant strain-displacement equations and proceed to step 7;
7. substitute the relevant column of $[R]^T$ into the required location in $[K]^T$, and remove that column from $[R]^T$;
8. record the substitution - this is the action required to be taken on the assembly set of equations;
9. return to step 4 and proceed as above until the number of one of the following is exceeded;
    a) boundary force-displacement equations to be replaced;
    b) strain-displacement equations available;
    c) relevant linear dependence relationships.

It is necessary to repeat the cycle after each substitution because of the possibility of alterations to the linearly dependent subsets. The information recorded can be used to construct a linearly independent set of assembly equations and thereby ensure a unique solution.

However, the above method could possibly be considered to be both time and space consuming from the computing aspect. For cases in which few substitutions are to be made, a set of empirical relationships can be constructed between the physical locations of the elements to which the strain-displacement equations relate and those of the nodes whose force-displacement equations are to be replaced, which effectively bypass the necessity to study the linear dependence/independence relationships involved. This is discussed further in the experimental section of the report.

2.33 The Solution Obtained from the Proposed Method

In the previous section it was shown that, under specific condit-tions, the adapted set of assembly equations of the proposed method is linearly independent and thus possesses a unique solution. The examination of the solution itself was, however, deferred to this section.

The simplest test of the proposed method is to compare its outcome with that of the conventional method, assuming a finite element model which is common to both systems. This can be performed in the following manner:

1. run a conventional analysis on the model and output the computed displacements in addition to the forces, stresses and strains;
2. compute the values for the strains at the elements' centroids, using the relationships $\{\varepsilon\} = [B]\{\delta\}$ as per Appendix A equation (vi), together with the displacements calculated in step 1 above;
3. run the proposed method on the model, replacing all those boundary force/displacement equations for which forces were specified in step 1, with relevant strain/displacement equations (cf. section 2.32) containing the strain values computed in step 2 above;
4. compare the solution sets of both methods.

Experimental runs performed as above have indicated that the two solution sets are identical. This can be mathematically verified using Nering's[46] observation that:

" .... if AX = B is the given linear problem with A an m x n

matrix/20.........

matrix and Q is any non-singular m x n matrix, then $A'X = B'$ with $A' = QA$ and $B' = QB$ is a problem with the same set of solutions." Let the conventional set of equations be represented by $[K]\{\delta\} = \{F\}$, and let the proposed set of equations formed by the substitution of strain/displacement equations into this set be represented by $[K']\{\delta\} = \{F'\}$. The linear algebraic reduction of $[K]\{\delta\} = \{F\}$ results in the set $\{\delta\} = [K]^{-1}\{F\}$, ie. the solution set of displacements. The values of the strains to be substituted to form $\{F'\}$ are calculated according to relationships of the form $\{\varepsilon\} = [B]\{\delta\}_e$. However, since the strain/displacement equations are in fact these selfsame relationships (cf. section 2.22), the strains appearing in $\{F'\}$ can be obtained simply from $[K']$ operating on the calculated displacements, ie. $\{F'\} = [K'][K]^{-1}\{F\}$. (Note that the rows of $[K']$ which describe force/discplacement equations are unchanged from those of $[K]$, and thus their multiplication into $[K]^{-1}$ merely results in their assumption of the identity form and the transcription of their relevant values in $\{F\}$ directly into $\{F'\}$). Since both $[K]$ and $[K']$ are non-singular square matrices, the matrix formed by $[K'][K]^{-1}$ is a non-singular square matrix. Having thus found the relationship between $\{F'\}$ and $\{F\}$, it remains to be shown that this relationship can also be applied to $[K']$ and $[K]$. This is trivial, ie.

$$\begin{aligned}[K'] &= [K]\,[K]^{-1}\,[K] \\ &= [K'][I] \\ &= [K']\end{aligned}$$

The two sets of equations thus have the same set of solutions.

The above test demonstrates the fact that the proposed and conventional sets of equations are equivalent when the strain data used in the former is identical to that obtained in the latter. It can be concluded that any errors induced into the values of the strains during their experimental measurement will generate corresponding inaccuracies in the solution set, the errors themselves being reflected exactly.

CHAPTER 3

THE DEVELOPMENT OF THE COMPUTER PROGRAMMES

3.1 INTRODUCTION

The computer programming of the proposed method has been dealt with in two phases, the first being the development of a two-dimensional programme for use in the experimental testing of the method (as covered in Chapter 4), and the second the construction of a three-dimensional programme based on this experience for future use in practical engineering applications. The shortage of time available for the thesis precluded the testing of the latter programme.

The programming aspect has commanded the most attention in this project, in terms of both time and effort. The prime concern has been the reliability of these programmes, and great care has been taken in attempting to minimise the effects of computing problems such as round-off error.

A factor to be emphasised is the inter-relationship between the development of the algorithms and the actual construction and testing of the programmes. For the sake of clarity these facets are presented as being distinct.

3.2 CONSIDERATION OF THE CONSTRAINTS IN THE PROGRAMME SPECIFICATION

The requirement that the method, and thus the programmes, be suitable for the localised analysis of areas of high stress gradients as described in the objectives (cf. section 1.2), results in the following constraints on the programming:

1) relatively small quantities of data are to be used;
2) general forms of stress-raisers need to be catered for;
3) a high degree of accuracy is required;
4) economy of computer time is required;
5) ease of handling of the data and programme by the user is necessary.

In addition,/22.........

In addition, the constraints of the linear elasticity model as specified in section 2.21 are to be applied, which results in the use of plane stress analysis in the two-dimensional case, and linear elasticity relationships in the three-dimensional programme.

The specifications which follow form a compromise between these factors.

3.21 The Type of Elements to be Used

The requirement that the programmes be capable of analysing general forms of stress-raisers, ie. stress concentrations, renders the use of specialised methods [19] and elements developed for cracks [20,21,22] and fillets [23] impracticable, as the development of a single programme incorporating these features is too complex to be considered in the project.

The modelling of stress concentrations with simple finite elements has been discredited because the flooding of the region of interest with small elements is both uneconomic and indecisive.[1,2,24,25] However, high-order curvilinear elements are considered eminently suitable for stress-concentration analysis in that they enable a relatively complex form to be represented by a small number of elements, and result in a "dramatic improvement" [1] in accuracy when the same number of degrees of freedom are used as in the case of a simple mesh.[1,26] Of the curvilinear elements available, the isoparametric element is the best documented,[1,25,26] and is thus chosen. Although it has been found that these elements give poor results when severly distorted from their basic shapes [26], this should be avoided by the judicious specification of the mesh.

For a description of the fundamentals of isoparamentric theory the reader is referred to Zienkiewicz.[1]

3.22 The/23..........

3.22 The Order of the Elements to be Used

The order of the elements refers to the order of the polynomial displacement function contained within the element shape function (cf. Appendix A equations i and iv). The use of high-order elements to model areas of high-stress gradient is strongly recommended, but must be justifiable on economic grounds. [1,11,26,27] A compromise between accuracy and economy must therefore be sought for.

Reference 26 contains a comparison of the accuracies achieved by various orders of isoparametric elements in the analysis of stress concentrations. From this, and on the explicit recommendation of references 24 and 26, the second order element, otherwise known as the linear-strain element, appears to be an optimum choice.

3.23 The Shape of the Elements

The choice of shape of the elements must compromise between:

1) the ease of modelling;
2) the ease of programming the mathematics;
3) the distortion of the element (cf. section 3.21).

The two- and three-dimensional elements are considered separately.

The rectangular element family has the advantage over the triangular family in the relative simplicity of its shape functions and numerical integration techniques. However, its inability to model certain complex shapes without considerable distortion compares very unfavourably with that of the triangles, which are eminently suited to the representation of complex plane shapes, [27] and the latter family is thus chosen for the two-dimensional problem.

In the three-dimensional situation the quadratic brick elements are superior to be tetrahedral family in all aspects, being easier to visualise and construct. In comparison tetrahedra are relatively inefficient and cumbersome. [25] The choice therefore

lies/24.........

2) the two-dimensional programme is to use quadratic isoparametric triangular elements;
3) the three-dimensional programme is to use quadratic isoparametric cubic elements;
4) the order of numerical integration to be used is 3.

3.3 THE ALGORITHMS OF THE PROGRAMMES

As the method proposed in the thesis is an adaption of the conventional displacement method, it follows that the computer programmes may likewise be evolved from the standard form. The construction of the algorithms from the basic formulation is the subject of this section.

3.31 The Displacement Method Algorithm

The model used as the basis in the project conforms to the systems described in references 1, 10, 27. The steps involved in the algorithm resemble closely those described in Appendix A, and are best presented in the flowcharted form of figure 1. The division of the programme into a main routine and three subroutines is of purely practical significance in the programming.

The generality of the steps presented in figure 1 precludes the detailing of sophistications such as those stipulated in section 3.2. However, other than the fact that the triangular elements require six nodes and the cubic elements twenty, the practical implementation of quadratic isoparamentic forms affects only the creation of the element stiffness matrices $[K']$ in the subroutine 'ELEMENT'. As the mathematical formulation of this aspect is well documented [1], a detailed description thereof is unnecessary.

3.32 The Algorithm for the Proposed Method

A resumé of the adaptions to be made to the standard system can

be stated/28.........

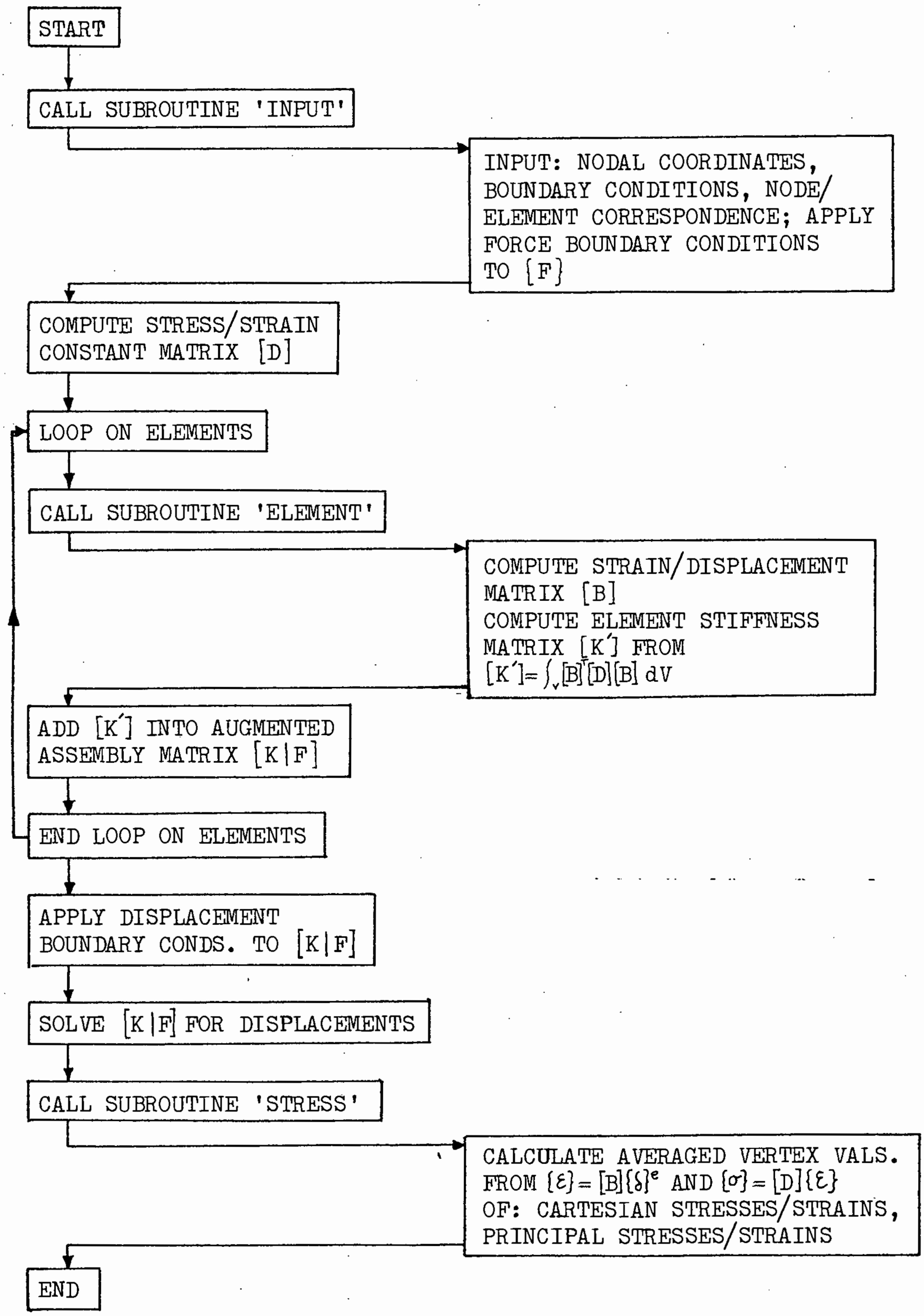

Figure 1.   Flowchart of the Displacement Method Model

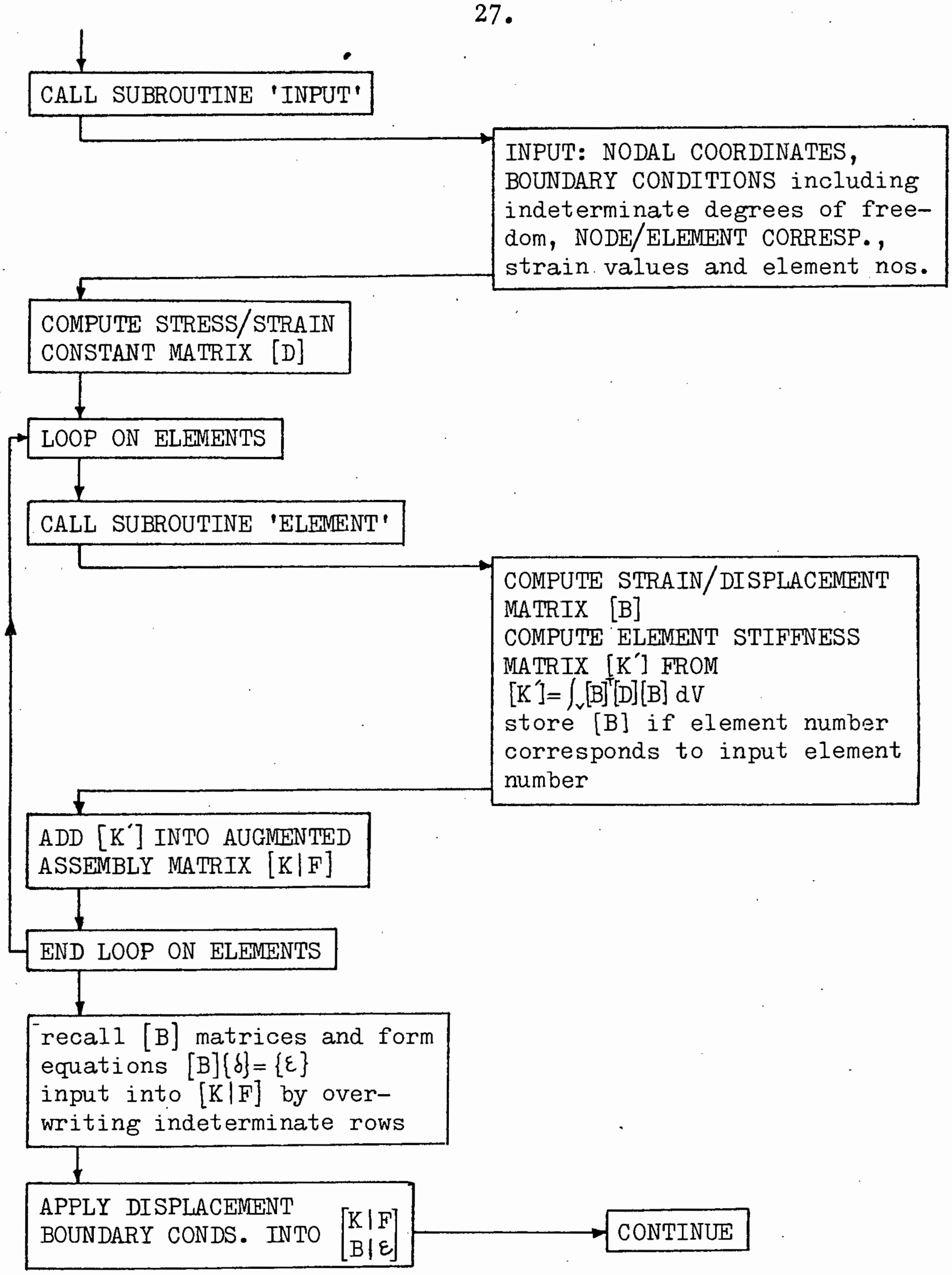

Figure 2. Flowchart of the Alterations to the Displacement Method Model Required for the Proposed Method

be stated as follows:

1) note the indeterminate degrees of freedom on the boundaries;
2) input the strain values and their relevant element numbers;
3) form the strain-displacement equations;
4) remove the indeterminate equations from the assembly;
5) input the relevant strain-displacement equations into the assembly.

In section 2.32 it was shown that the choice of the strain-displacement equations must be based on considerations of the linear dependence/independence relationships between these equations and the force-displacement equations they are to replace. Two methods were referred to whereby this could be achieved:

1) by the use of multiple reductions to the row-echelon form of the augmented transposed assembly matrix;
2) by the use of empirical rules appertaining to relative locations within the mesh.

The development, within the limited time available, of the theory of the method from the simple model in which these considerations were not made (cf. section 2.23) to the more sophisticated theory of section 2.32, is reflected in the development of the programming. Since the programmes were initially constructed on the basis of the simple theoretical model, it is evident that the second of the above-listed techniques for determining relationships is the most convenient to incorporate: it requires no further developments in programming, particularly with regard to the coping with large computing time and space factors. The lack of time available for this thesis has prevented the coding of the more exacting first technique for anything other than a small test programme. The emphasis in the remainder of this chapter is thus placed on the implied use of the second technique.

From figure 1 it can be seen that relatively minor changes are involved in programming the five steps listed at the beginning of this sub-section. The indeterminate boundary degrees of freedom can be marked during the specification of the boundary conditions in the subrountine 'INPUT', ie. their status is included in the data-pack submitted to the programme. The strain values and their relevant element numbers may be input in the same manner. In the formation of the strain-displacement equations

$$\{\varepsilon\} = [B]\{\delta\}_e$$

the matrix $[B]$ is required for each relevant element (or every element if technique 1 is to be applied). As the matrix $[B]$ is formulated in subrountine 'ELEMENT' for each element in the mesh, the matrices of the relevant strain elements can be singled-out at this stage and stored for the later construction of the equations. The removal of the force-displacement equations from the assembly and their subsequent replacement by the relevant strain-displacement equations is achieved by merely overwriting the indeterminate rows with the replacing equations.

The alterations to the standard model are flowcharted in figure 2, with only the relevant secion of the programme being depicted. The uncharged steps (cf. figure 1) are typed in capital letters and the modifications are in lower case.

Note that if technique 1 is to be used, the system differs from the above in that the algorithm presented in section 2.32 is included into the programme prior to the step of "input into $[K|F]$ by overwriting indeterminate rows".

3.33 <u>The Construction of the Strain-Displacement Equations</u>

A more detailed description of the strain-displacement equations than that provided in the previous sub-section is necessary, as the following two points require clarification:

1) the assurance that the withdrawal of the $[B]$ matrix during the construction of the stiffness matrix can be achieved without compromising the quadratic isoparametric formulation used;
2) the insertion of the centroid coordinates into the $[B]$ matrices.

The first/30.........

The first point can be considered from the point of view of the status of the [B] matrix when it is transferred from the sub-routine 'ELEMENT'. This matrix is defined at a particular point i of the finite element mesh as consisting of the derivatives of the shape functions specified at that point by the global coordinates, ie.

$$[B_i] = \begin{bmatrix} \frac{\partial N_i}{\partial x} & 0 & 0 & \frac{\partial N_i}{\partial y} & 0 & \frac{\partial N_i}{\partial z} \\ 0 & \frac{\partial N_i}{\partial y} & 0 & \frac{\partial N_i}{\partial x} & \frac{\partial N_i}{\partial z} & 0 \\ 0 & 0 & \frac{\partial N_i}{\partial z} & 0 & \frac{\partial N_i}{\partial y} & \frac{\partial N_i}{\partial x} \end{bmatrix}^T$$

However, the use of a high-order element system results in the shape functions being specified in terms of local coordinate systems ξ, η, ζ, and a transformation of the derivatives is required. This is achieved by means of the Jacobian matrix [J] , ie.

$$\begin{Bmatrix} \frac{\partial N_i}{\partial \xi} \\ \frac{\partial N_i}{\partial \eta} \\ \frac{\partial N_i}{\partial \zeta} \end{Bmatrix} = \begin{bmatrix} \frac{\partial x}{\partial \xi} & \frac{\partial y}{\partial \xi} & \frac{\partial z}{\partial \xi} \\ \frac{\partial x}{\partial \eta} & \frac{\partial y}{\partial \eta} & \frac{\partial z}{\partial \eta} \\ \frac{\partial x}{\partial \zeta} & \frac{\partial y}{\partial \zeta} & \frac{\partial z}{\partial \zeta} \end{bmatrix} \begin{Bmatrix} \frac{\partial N_i}{\partial x} \\ \frac{\partial N_i}{\partial y} \\ \frac{\partial N_i}{\partial z} \end{Bmatrix} = [J] \begin{Bmatrix} \frac{\partial N_i}{\partial x} \\ \frac{\partial N_i}{\partial y} \\ \frac{\partial N_i}{\partial z} \end{Bmatrix}$$

The isoparametric system of mapping the global variables x,y,z in terms of the global nodal coordinates is then implanted into [J]. The [B] matrix can then be expressed in the transformed terms obtained from

$$\begin{Bmatrix} \frac{\partial N_i}{\partial x} \\ \frac{\partial N_i}{\partial y} \\ \frac{\partial N_i}{\partial z} \end{Bmatrix} = [J]^{-1} \begin{Bmatrix} \frac{\partial N_i}{\partial \xi} \\ \frac{\partial N_i}{\partial \eta} \\ \frac{\partial N_i}{\partial \zeta} \end{Bmatrix}$$

It is thus evident that the [B] matrix can be related to the global system of strains and displacements on completion of these steps without any difficulty, and it is therefore in this transformed form that it is stored during 'ELEMENT'.

The second point requires the specification of the [B] matrix at the exact location in the finite element mesh at which the strain

components/31...........

components are experimentally assessed. This is achieved simply by setting the variables (expressed in local coordinates) in the shape functions to relevant values, eg. in the triangular element case the local area coordinates are each set at $\frac{1}{3}$. The three-dimensional case is complicated by the need to specify the element face on which the strains are measured. This is done by means of a coding system which uniquely identifies the face in terms of the local coordinates: the code number is input simultaneously with the strain values and the element number.

Thus the strain-displacement equations generated are fully capable of relating the strain components measured at centroid or on a surface face of an element to the global displacements of the nodes of that element.

3.4 THE HANDLING OF THE ASSEMBLY MATRIX

The programme coding of the proposed method is a relatively straightforward task, and a detailed description is thus not presented in this report. However, the handling and solution of the large sets of assembly equations on the UNIVAC 1108 computer at the University of Cape Town have presented some difficulties which do warrant mention.

It must be noted that the present discussion applies to the programming of the method based on the algorithm flowcharted in figure 1 and 2. However, although the techniques described in this section have been developed for the handling of the set of assembly equations subsequent to substitutions, it should be evident to the reader that these techniques can be readily adapted for use in programming the multiple reduction system used for determining linear dependence/independence relationships (cf. section 2.32).

3.41 The/32..........

3.41 The Nature of the Set of Assembly Equations

Before describing the methods used to deal with the equations, certain points concerning the nature of the assembly equations must be made, namely:

1) the matrix is unsymmetric as a result of the incorporation of the strain-displacement equations;
2) elements on the leading diagonal of the matrix prior to solution are not necessarily non-zero (cf. figure 3);
3) the order of magnitude of the strain-displacement equations, ie. the necessity for row scaling, requires assessment.

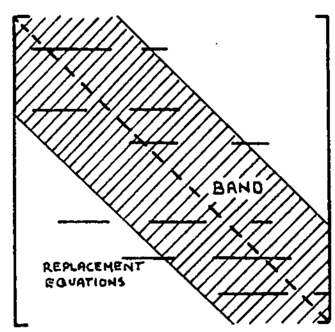

Figure 3. A Schematic Representation of a Typical Set of Equations Prior to Their Solution

These factors need to be taken into account in the solution technique used.

3.42 The Problem of the Matrix Handling and Solution

The two-dimensional programme was initially coded to utilise a packaged Gauss-Jordan partial-pivoting elimination technique (GJR) [30] for the solution of the assembly matrix. This requires the full matrix to be core-resident. While this system proved to be suitable for the small test-meshes described in section 3.5, it was soon discovered that the storage requirements of meshes of practical size, eg. 300 degrees of freedom, exceeded by far the 65 000 words of core made available by the FORTRAN $\bar{\underline{V}}$

compiler. It was thus decided to implement an economic and storage-saving technique for the handling and solution of the equations.

A search was made for an existing sub-programme capable of dealing with the problem. This proved to be unsuccessful as, to quote Key,[35] " ..... the overwhelming majority of available computer programmes for the solution of large algebraic systems seem to be restricted to full, symmetric or banded arrays." The distortion of the assembly set caused by the strain-displacement equations (cf. section 3.41) rendered impractical such approaches as the frontal [1,31,32], sequential [33], sparse matrix and sub-structural.[34]

In the absence of a suitable method the decision was taken to develop a scheme suited to the problem in hand. It is unfortunate that at the time of coding the programmes the writer was unable to obtain a copy of the paper by Key [35], as the sub-programme presented therein complies entirely with the problem requirements.

An extraneous factor to be considered prior to the development of the matrix methods was the question of row scaling [16] mentioned in section 3.41. As described in section 3.5, this question was tested on a small mesh using packaged Gauss-Jordan elimination schemes, and it was found that the scaling of the strain-displacement rows to the order of magnitude of the force-displacement rows, achieved by multiplying through by a factor of 10^{10}, successfully eliminated the errors arising from computer roundoff problems. [16,30]

3.43 The Schemes Developed for Handling and Solving the Equations

The development of solution schemes has been intimately linked with the requirements imposed by the sizes of the finite element meshes being dealt with. The storage requirements of the two-dimensional meshes are not overtly severe due to the initial constraint

of developing/34..........

of developing the method for small meshes only. Thus a mesh of 250 nodes and 175 elements would be considered to be the maximum size applicable. The three-dimensional case does present problems, as the fact that 80 degrees of freedom exist per element, together with the very large bandwidths, [36] impose heavy restrictions on the number of elements capable of being handled.

Two devices are available for overcoming the problems of storage:

1) the compacting of the matrix and the use of pointer matrices to indicate row and column locations;
2) the use of direct-access peripheral storage files which provide adequate space for storage.

In using these devices consideration of the four phases of matrix handling involved in the method must be taken into account, namely:

1) the adding of the element stiffness matrices into the assembly set;
2) the substituting of the strain-displacement equations;
3) the imposing of the displacement boundary conditions, if any;
3) the solving of the set of assembly equations for the displacement vector.

Gaussian elimination with sequential pivotting was chosen as the basic technique with which to operate as it involves the least number of arithmetical operations of the methods available for matrix solution [16], and is the easiest to programme. Although it does have the disadvantage of generating long non-zero row lengths [35], precedence exists for its usage in matrix schemes. [1,31,32,33,37]

The schemes developed have been based on a strategy devised by the writer, which is presented here in point form.

1) An in-core pointer matrix is required which has a length dimension equal to the number of degrees of freedom of the assembly set, and a breadth corresponding to the anticipated nodal bandwidth.
2) The assembly matrix is created either in-core or in

peripheral storage and possesses the same length dimension as the pointer matrix, but has as its width the anticipated bandwidth of degrees of freedom, plus one extra column for the augumented form.

3) The adding of the element stiffness matrices into the assembly matrix is controlled by the pointer matrix. The pointer matrix itself stores the column locations of the coefficients as they would appear in the full assembly matrix. However, it is compiled on a basis of left-justified rows of non-zero integers, and the physical location of the pointer value within the abridged matrix is used to locate the real coefficient value within the assembly matrix.
4) The strain-displacement coefficients are overwritten into the assembly set, their pointers being stored in the same manner as above. The values of the strain measurements are placed in the right-most column of the assembly matrix.
5) Both matrices are ordered, row-by-row, into ascending column values in the pointer matrix. This ordering is performed simultaneously so as to ensure that the columnwise correspondence is not destroyed.
6) The displacement boundary conditions, if any, are imposed by setting the respective coefficent to unity and the associated coefficents to zero, as described by Zienkiewicz[1].
7) The solution of the assembly equations is controlled by the pointer matrix which is updated at every step. The location of pivots and secondary rows, and all arithmetic operations involved in Gaussian elimination,are referenced from it. The solution of the set of equations, ie. the displacement vector, is resident in the right-hand column of the assembly matrix at the conclusion of the assembly procedures.

Two main schemes based on this strategy have been developed, namely;

1) the in-core system, in which the assembly matrix is created in core;
2) the peripheral storage system, in which the direct-access storage facility has been utilised to store the assembly

matrix./36.........

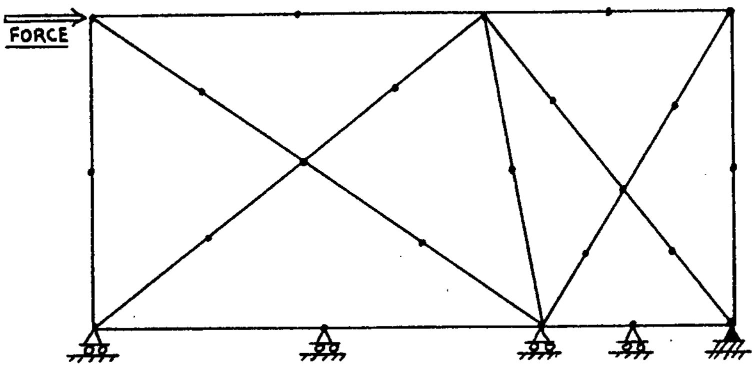

Figure 4. A Finite Element Model used for Programme Testing

However, inconsistent performance of this technique led to the use of another package (LSIMEQ) [30] which enables control to be exercised over the error flag for determining the condition of the matrix.

A series of runs was made using various settings of the flag on matrices known to be singular, and on well-conditioned cases, and it was determined that an error level due to roundoff error exists at an order of 10^8 less than the value of a representative element of the matrix.

The decision was thus made to increase the order [16] of the loading equations by a factor of 10^{10}.

3.52 The Type of Strain-Displacement Equation to be Used

In chapter 2 it was shown that the loading equations can be written either separately or in a summed form.

A series of tests using the model in figure 4 confirmed the assumption that no difference in computational accuracy exists between the two methods. The choice of equation type can therefore be made in accordance with the accuracy of the experimental strain values being used. For the remainder of this project the loading equations were programmed in their separated form.

3.53 The Execution Times of the Matrix Handling Methods

A series of runs was made using the model in figure 4 to compare the execution times and accuracies of the two schemes presented in section 3.43 with the packaged [30] Gauss-Jordan technique. The results are given in table 1.

solution method	execution time (seconds)
packaged solution	7.993
incore scheme	6.517
peripheral storage scheme	135.368

Table 1. A Comparison of Execution Times

The dramatic increase in solution time of the peripheral storage technique is clearly demonstrated. The results obtained by the three systems proved to be equivalent to the fourth significant place.

3.6 A SUMMARY OF THE PROGRAMMES DEVELOPED

A detailed description of the programmes developed in this project is thought to be unnecessary. However, a very brief summary of the characteristics of the main programmes is presented in this section.

The main programmes have the following features in common:

1) adherance to the programme constraints listed in section 3.2;
2) a structure comprising of a main routine and three sub-

routines, as described in figure 2;

3) a matrix handling and solution scheme embodied in the main routine, and utilising the internal subroutine facilities available in the FORTRAN $\overline{\underline{V}}$ programming language;

4) a "stress-averaging" scheme whereby the strains are evaluated element-wise at a vertex node and are then averaged for that node, before being transformed to the nodal stress value.

Four programmes have evolved during the project, each refined for an area of application. The programmes are listed, together with their usage, under their code-names as follows:

1) FEMSGG - programme developed for small and medium sized two-dimensional meshes, and utilising the in-core assembly matrix scheme;

2) FEMSGT - programme developed for small two-dimensional meshes, utilising the in-core assembly matrix scheme and incorporating coding of the algorithm of section 2.32;

3) FEMSGL - programme designed for large two-dimensional meshes, and incorporating the peripheral storage scheme for the assembly matrix;

4) FEMD3 - programme developed for the three-dimensional mesh analysis, and utilising the peripheral storage scheme.

The use made of these programmes during the project is described in the following chapter.

CHAPTER 4

THE EXPERIMENTAL TESTING OF THE METHOD

4.1 INTRODUCTION

As has been mentioned previously in this report, the aspects of theory development, programme development and experimental testing have been closely intertwined in developing the proposed method. The separation of these aspects into their relevant chapters has been performed for the sake of clarity, and their order of presentation within this thesis should not be interpreted as being chronologically accurate, especially as much of the programming and experimental work actually preceded the full development of the theoretical model. In order to simplify presentation, and for the sake of completeness of this report, it has been decided to describe the major items of the experimental testing in the sequence in which they were performed, allbeit that the initial work is outdated with respect to the later developments in the theory described in Chapter 2.

The experimental testing of the proposed method has progressed through four major phases:

1) the testing of a small data model using programme FEMSGG;
2) the construction of physical data models and their testing using programmes FEMSGG and FEMSGL;
3) the retesting of the small data model using programme FEMSGT;
4) the retesting of the physical data models using programme FEMSGG.

The first two of the above phases were based on the simple theoretical model described in section 2.23, ie. with no considerations of the linear dependence/independence relationships being made. The method appeared to work well in phase 1, and phase 2 was consequently executed: this however yielded inconsistent and often unintelligible results which clearly indicated that the theoretical model was incomplete. Subsequent research of strain-displacement equations. The choice of these latter equations was taken as being arbitrary and was thus based on convenience.

4.22 The Testing

The testing comprised a set of six runs incorporating variations in the manner in which the boundary conditions were specified. The runs are listed in table B1 of Appendix B.

The loading data for the series was obtained by applying an arbitrary force to the constrained mesh, and computing the strains at the element centroids by conventional means. This run, FEMS1, was followed by the other five runs in which the loading and displacement data were combined in the following forms, viz:

1) run FEMS2: fixed displacement boundary conditions specified as in FEMS1; force-displacement equations, including that containing the initial loading force, arbitrarily removed and random strain-displacement equations inserted.
2) run FEMS3: three fixed displacement boundary conditions arbitrarily specified, the equations pertaining to the fixed-displacement boundary conditions of FEMS1 removed and replaced by random strain-displacement equations; the force-displacement equation containing the initial loading force not disturbed.
3) run FEMS4: no fixed-displacement boundary conditions specified, all equations pertaining to the fixed-displacement boundary conditions of FEMS1 removed and replaced by random strain-displacement equations; the force-displacement equation containing the initial loading force not disturbed.
4) run FEMS5: no fixed-displacement boundary conditions specified; all equations pertaining to the fixed-displacement boundary conditions of FEMS1, and the force-

displacement equation containing the initial force, removed and replaced by random strain-displacement equations.

5) run FEMS6: no fixed-displacement boundary conditions specified; no strain-displacement equation substitutions made; the force-displacement equation containing the initial loading force not disturbed.

For the reasons discussed in section 2.212, it is evident that runs FEMS4, FEMS5 and FEMS6 should have resulted in singular matrices and hence infinite numbers of solutions. However, due to the finite arithmetic characteristics of the computer, solutions were in fact obtained. These runs are therefore reported to illustrate the potential hazard of this phenomenon in providing misleading results.

4.23 Analysis of the Results

In retrospect, it is evident that none of the runs made in this series could be classified as typical of the intended utilisation of the proposed method. These runs did, however, provide important insights into the functioning of the method.

A programme was written to compare, on a percentage error basis, the results of the various runs in terms of displacements, stresses and strains, using FEMS1 as the datum. Tables containing these comparisons for the displacements and for σ_x, a representative quantity, are provided in Appendix B.

From tables B2 and B3 it can be seen that run FEMS2 validated the basic premise of the proposed method; that the force-displacement equations conventionally used to specify loading data can be replaced with strain-displacement equations containing equivalent loading data. The replacement of more than the minimum required number of equations did not significantly effect the outcome of the run.

Run FEMS3 similarly involved the removal of conventionally specified loading data, this time in the form of the fixed-displacement boundary conditions. The specification of alternative fixed-displacement boundary conditions resulted in the mesh undergoing a rigid-body motion with respect to the frame of reference used in FEMS1. This had little effect on the computations of the stresses and strains, as these are derived from relative and not absolute displacements. The run was deemed significant in that it demonstrated the ability of the proposed method to accurately solve for stress and strain fields irrespective of the manner in which the body is physically located in space by means of the displacement constraints.

The accuracy of the stress and strain results of FEMS4 and FEMS5 appeared to indicate that the proposed method is capable of bypassing the necessity to specify the minimum number of boundary constraints. As this was known to be contradictory to theory (cf. section 2.212), it was deduced that roundoff errors inherent in the reduction processes effectively increase the rank of the assembly matrix and thereby artificially locate the body in space: the mesh undergoes a limited amount of rigid-body motion as it assumes its location, but the relative displacements and hence the stresses and the strains are unaffected. Run FEMS6 was made to determine the magnitude of this roundoff error effect in a conventional case of singularity: the results obtained (cf. tables B2 and B3) are clearly indicative of singularity. Rather than support the hypothesis of roundoff error as the cause of the accurate results of FEMS4 and FEMS5, run FEMS6 thus served to confuse the issue by appearing to indicate that, by comparison, the former two runs suffered no effects of singularity or ill-conditioning, and the necessity for displacement constraints could therefore be dispensed with in the proposed method. It was only in the second phase of testing that this was conclusively proved to be a fallacy.

Analysing/45.........

Analysing the results of the series in retrospect of the later developments in the method, it is evident that the apparent contradictions in the results can be explained in terms of the linear dependence theories of section 2.32, and the finite arithmetic errors inherent in the computations. The inaccuracies present in the results of runs FEMS3 and FEMS2 stemmed from the choices made of the strain-displacement equations to be substituted for the force-displacement equations: ignorance of the necessity for linear dependence relationships between the relevant equations resulted in these choices being made in a random manner. The similarity of the results of runs FEMS2, FEMS3, FEMS4 and FEMS5 indicates that, in fact, the former two runs should likewise have produced ill-conditioned or possibly even singular results had it not been for the presence of roundoff errors in the reduction processes. The apparent accuracy of the results may be attributed to the very small size of the mesh (and assembly matrix), as this phenomenon of the masking of the evidence of singularities was not repeated in the medium and large mesh cases of the second phase of testing.

The conclusion thus reached at the end of this first phase of testing was that the method itself was capable of functioning, although the inconsistancies in the results, especially in the case of displacement constraints, were inexplicable in terms of the existing theory.

4.3 PHASE TWO: TESTING THE SIMPLE THEORETICAL MODEL ON PHYSICAL DATA MODELS

The objective of this phase of the experimental testing was to assess the capability of the proposed method (in the form of programmes FEMSGG and FEMSGL) in analysing real cases of stress raisers.

Three physical models were constructed, and their stress fields under loading were measured in the laboratory using the reflection polariscope technique. The strains thus obtained were subsequently used as the input loading data for the finite element analysis of these cases using the proposed method. It was intended to compare the two sets of results in order to provide an indication of the effectiveness and accuracy of the proposed method.

4.31 The Models

This section deals with the choice and design of the physical and data models. The theoretical model on which the programmes were based was unchanged from that described in section 4.21.

4.311 The choice and design of the physical models. The attributes required of the models can be listed as follows:

1) that the models be two dimensional;
2) that the stress concentrations modelled be of a conventional nature;
3) that the manufacturing of the physical models be simple;
4) that the models be suited to the experimental techniques used to evaluate the strains.

As the models were to be loaded using the Amsler tensile testing machine at U.C.T., it was decided that, for the sake of simplicity, the choice of models would be limited to plane-stress (plate) cases with tensile loading. From the various categories of stress concentration problems falling within this limitation[38], the cases of a centralised hole in a plate, and fillets in a plate, were chosen.

It was decided to build three models:

1) a plate with a central hole, to be used for large-scale mesh testing;
2) a plate with large fillets, to be used for a medium-sized mesh test;

3) a plate/47.........

3) a plate with sharp fillets, to be used for a range of meshes.

Recourse was made to literature available in the field of stress concentrations for the specification of model configurations of common interest. As the detailed design of the models is of secondary importance in this report, the specifications will merely be summarised as follows:

1) model FEM1: a plate with a central hole (figure 5a), having a hole-diameter to plate-width ratio of 0,3, and an anticipated maximum stress concentration factor[32,38,39] of 4
2) model FEM2: a plate with a sharp fillet (figure 5b), with the ratio of the larger width to the smaller of 1,2, having a fillet-radius to smaller-width ratio of 0,02 and an anticipated maximum stress concentration factor [40] of 3.
3) model FEM3: a plate with a large fillet (figure 5c), with the ratio of the larger width to the smaller of 4, having a fillet-radius to larger-width ratio of 0,375 and an anticipated maximum stress concentration factor [41] of 1,15.

The material used for the models was 4,4mm thick mild steel plate.

4.312 <u>The design of the data models.</u> The design of the finite element meshes of the models was performed at this stage of the experimental testing to facilitate the construction of orderly meshes. It should be noted that this proceedure requires that experimental readings of strains be taken at specific points of the physical model. An alternative proceedure would be to measure the strains at arbitrary points on the physical model and subsequently construct the mesh in such a way as to have these points coincide with the centroids.

Because of the limited time available for the project, automatic mesh generation [42-44] facilities were not coded into the programmes. The meshes used were thus hand-drawn, and based on meshes used in similar cases described in the literature.[1,4,11,26,45]

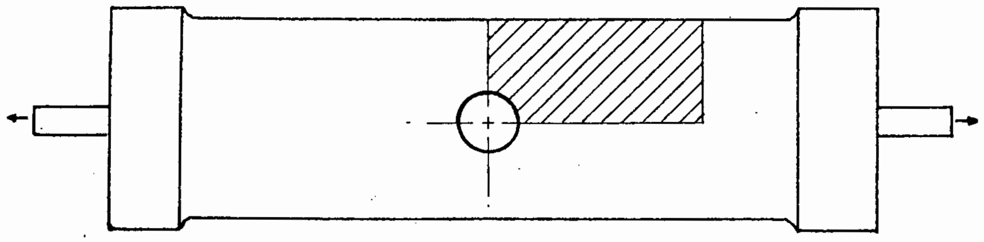

(a) model FEM1

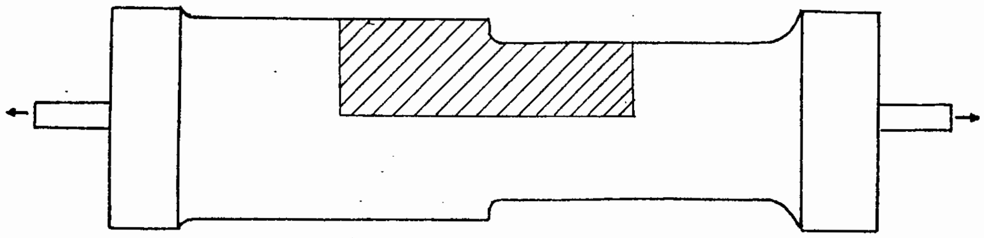

(b) model FEM2

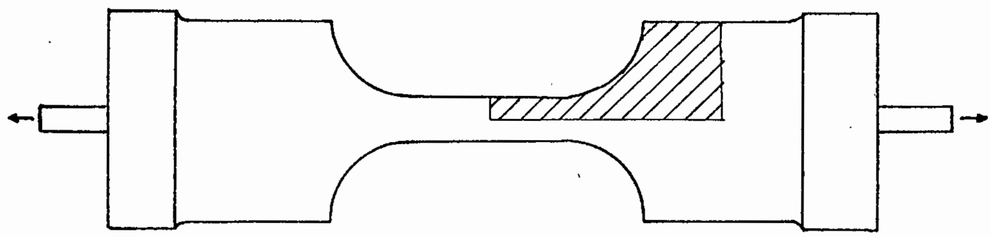

(c) model FEM3

Figure 5. The Physical Models, Illustrating the Method of Loading and the Finite Element Mesh Locations

A computer graphics programme, written by Mr. J.E. Newmarch, was used as a visual aid in checking the data, and copies taken of the displays are presented in Appendix C.

Two factors of the mesh design warrant mention, namely:

1) the axes of symmetry of the models were used wherever possible to minimise the overall size of the meshes;
2) the numbering of the nodes and elements was not subjected to any bandwidth controls [1,44], as this was deemed unnecessary due to the use of the matrix-handling scheme (described in section 3,34), which provides for the storage of non-zero values only.

The specifications of the data models (meshes) can be listed according to their respective physical models.

1) Model FEM1: one data model, labelled FEM1, of 163 nodes and 68 elements.
2) Model FEM2: four data models of the following specifications:
   FEM2 comprised of 218 nodes and 91 elements;
   FEM2A comprised of 156 nodes and 63 elements;
   FEM2B comprised of 90 nodes and 35 elements;
   FEM2C comprised of 79 nodes and 30 elements.
   The relationships between these data models can be described in set notation as: $FEM2 \supset FEM2A \supset FEM2B \supset FEM2C$.
3) Model FEM3: one mesh, labelled FEM3, of 103 nodes and 40 elements.

4.32 The Laboratory Testing

This section provides a brief description of the experimental tests which were run on the physical models for the purpose of:

1) evaluating the strains to be used as the input data for the computer runs of the proposed method;
2) evaluating the stress fields for comparison with those resulting from the computer runs of the proposed method in

order to evaluate the effectiveness and accuracy of the method.

A detailed treatment of the testing is not provided in the report: the activities involved are merely summarised.

3.321 <u>The experimental means of strain measurement.</u> Of the means available for the experimental determination of strains[39], the methods of strain-gauging and photelastic coating are the most advantageous in terms of accuracy and ease of handling. The latter method was chosen for use in the thesis, being particularly suited to the large number of measurements required.

The reflection polariscope used was a Photolastic Model 030, owned by the South African Railways. The use of accessories 033 for oblique incidence measurement, and 232 uniform field compensator for a direct compensation readout of the fringe nodes, enabled the direct evaluation of the individual principal strains and their directions.

A high-sensitivity photoelastic coating for the models was required in order to maximise the stress-optic effect [39] which is inherently low in the materials used in this form of testing. The material chosen was 2,13mm thick sheeting of type Photolastic PS-2B, having a fringe value f of 1040×10^{-6}m/m/ fringe order. The adhesive used was a reflective type, Photolastic PC - 1.

The Young's modulus and Poisson's ratio for the steel plate used in the models were determined by means of coating a sample strip with the photoelastic material, loading it in tension in the Amsler tensile testing machine, and measureing the strains obtained from a series of applied loads. The appropriate[3,39] stress/strain curves provided values of 2.052×10^{2} GNm^{-2} for the Young's modulus and 0,35 for Poisson's ratio. The yield point of the steel was also tested for, and found to be 320 MNm^{-2}. Using this value and the fringe value f of the

material,/51.........

material, it was thus ascertained [39] that the maximum fringe order which could be obtained was 1,44.

4.322 <u>The testing of the models.</u> The maximum permissable tensile loads for the models were calculated from the yield stress and the stress concentration factors listed in section 4.311. The maximum loading range for the models was thus found to lie between three and four tonnes.

The model coatings were found to exhibit birefringent patterns prior to loading as a result of:

1) an uneven distribution of adhesive between coating and model;
2) changes in ambient temperature subsequent to adhesion causing thermal expansion stresses in the plastic;
3) residual thermal stresses at the machined edges of the coating;
4) hygroscopy.

It was thus necessary to take two sets of readings, the first being in the unloaded condition and the second in the loading condition, and to subtract the effects of the first from the second.

The strains were measured at the centroids of elements chosen at random in the mesh, as it proved to be too time-consuming to measure each and every element. Model FEM3 was accidently overloaded during the testing and plastically deformed, thereby proving useless for further investigation. The strain values measured in models FEM1 and FEM2 were converted to Cartesian components to match the requirements of the programmes, and were plotted using a computer graphics programme written by Mr. J.E. Newmarch. Copies of these displays are presented in Appendix C.

4.323 <u>The results obtained from the testing.</u> The majority of the strain values obtained correspond to those published in the literature on which the models were based (cf. section 4.311). Certain isolated values appear to be obviously erroneous, and these errors can be attributed to:

1) the awkwardness of the oblique incidence attachment occasionally resulted in a poor light distribution on the point concerned;
2) the factors contributing to prestressing (as listed in section 4.322) also effected the stressed condition.

The values which were obviously in serious error were not automatically discounted from further use, as it was felt that such data represented a typical set of experimental readings. The data output by the programmes was expected to coincide with the strain values input, and these errors thus reproduced.

4.33 The Computer Testing

This section deals with the computer runs made in testing the data models of the series.

4.331 Data model FEM1. The attempts made to run programmes FEMSGL and FEMSGG on this model proved unsuccessful. It was discovered that the enormous amounts of input/output time of the former programme required an estimated run-time of 6,5 hours. Programme FEMSGG was coded to use the extended storage facility (cf. section 3.43), but an untraced problem with the addressing of the arrays prevented its usage.

Due to the limited time available for the project, the decision was made to scrap the use of the model.

4.332 Data model FEM2. The runs using this model met with the same obstacles as those described for FEM1, except that in this case, the estimated run-time of FEM2 was set at 8,7 hours.

The model/53.........

The model was similarly deleted from the testing schedule.

4.333 Data model FEM2A. A series of four runs was made in testing this model. The programme used was FEMSGG, coded for extended storage, and the loading data was comprised of the experimentally determined strains. The runs are listed in table D1 of Appendix D.

The necessity to make more than the single run initially intended arose from the meaningless results (in the context of the contemporary theory) that were obtained. The three extra runs were made in an attempt to assess the cause of the singularity which was occurring and to bypass the problem if possible: these runs proved unsuccessful, however.

The analysis of the results of the series is presented in section 4.3.

4.334 Data model FEM2B. A series of five runs was made in testing this model. The programme used was FEMSGG, and the loading data was comprised of the experimentally determined strains. The runs are listed in table E1 of Appendix E.

This series of runs was made in an attempt to assess the effect of various combinations of loading elements on the outcome of the analysis: all the runs contained singularities, however. It should be noted that the absence of displacement constraints in four of the five runs was a result of the confused thinking on this subject which existed at the time (cf. section 4.23).

The analysis of the results of the series is presented in section 4.3.

4.335 Data model FEM2C. A series of eight runs was made in testing this model. The programme used was FEMSGG, and the loading data was comprised of the experimentally determined strains. The runs are listed in table F1 of Appendix F.

The objectives of this series of runs were twofold: firstly, to assess the influence of various combinations of displacement constraints and loading element specifications on the outcome of the analysis; secondly, to examine the question of the necessity for the specification of fixed-displacement boundary conditions. The first four runs were thus made with various combinations of loading elements and displacement constraints, and the second four comprised a repeat of these combinations of loading elements without the displacement constraints being specified.

The analysis of the results of the series is presented in section 4.343.

4.336 Data model FEM3. A series of nine runs was made in testing this model. Although no experimentally obtained loading data was available (cf. section 4.322), it was decided to apply arbitrary forces to the mesh, compute centroid strains in the conventional finite element manner, and use these values for further testing. The programme used was FEMSGG, coded for extended storage. The runs are listed in table G1 of Appendix G.

The series was made in an attempt to assess the interelationship between the locations of the constrained displacement boundary conditions and those of the loading elements.

The analysis of the results of the series is presented in section 4.344.

4.34 Analysis of the Results

The presentation of the general conclusions concerning the second phase of testing is preceded in this section by the analyses of the individual series of runs performed on the data models.

Detailed analysis has been precluded from the report for the sake of economy, but it is felt that sufficient data is presented in Appendices C to G to enable the reader to study the runs and their outcomes.

4.341 Data model FEM2A. All four runs of this series proved to be subject to singularities, and the stress and strain results were meaningless with, for instance, strains of the order of 10^{10} being obtained.

The displacement vector generated by the reduction of the assembly matrix was output for each run in an attempt to gain an insight into the problem. Excessive displacements were found to occur at certain nodes, and an analysis of this behaviour, in relationship to the locations of the elements pertaining to the strain-displacement equations, was performed in an attempt to assess the causes of the aberrations (cf. table D2 of Appendix D). It was found that the greatest errors in displacements occurred at nodes which were related to the boundary force-displacement equations being removed and yet were remote from the elements pertaining to the strain-displacement equations used in the substitutions. The effect was particularly noticeable in the case of the nodes of element 58, where nine of the twelve degrees of freedom were specified as indeterminate and their force-displacement equations removed, without any strain-displacement equations relating to the elements in the vicinity being utilised.

It was concluded that the rank deficiencies existing in the runs could possibly be avoided by the judicious choice of loading elements in the vicinity of the boundary nodes whose force-

displacement/56.........

displacement equations were to be replaced. This appeared to be of particular importance in the case of the boundary nodes of corner elements.

In the light of the subsequently developed theory, this conclusion has proved to be correct. It is evident that no linear dependent relationships existed between the boundary nodes which exhibited the errors and the strain-displacement equations with which they were substituted, and the resulting set of assembly equations was thus linearly dependent and singular.

It should be noted that although run FEM2A4, made without boundary constraints, did evidence a slight deterioration in results when compared to FEM2A1, the poor condition of all the results prevented the conclusive settlement within this series of the question of fixed-displacement boundary conditions.

4.342 Data model FEM2B. All five runs of this series proved to be subject to singularities, a result which may be attributed to the lack of displacement constraints (in four of the runs) as well as to the inadequate choice of loading elements. Due to the roundoff error effect of artificially locating the unconstrained body in space (discussed in section 4.23), the series may still be considered to be valid for the assessment of the effect of various combinations of loading elements on the outcome of the analysis.

The use of a graphics programme to display the results greatly facilitated the analysis. These displays, together with comments, are presented in Appendix E.

It was concluded that the corners in the boundaries of the mesh were the focal points of the errors, and that the specification of strains in the elements containing these nodes overcame the problems. In retrospect of the later developments in theory, it is evident that this conclusion was correct, allbeit that the stipulation regarding the choice of elements must necessarily be extended to apply to all boundary nodes.

It should be noted that the order of magnitude of the errors in the results of this series are considerably lower than those of the FEM2A series. This may be attributed to the fact that the FEM2B model is smaller and thus the loading elements used, although randomly chosen, lay closer to the boundaries and thus possessed stronger linear dependence relationships.

4.343 Data model FEM2C. All eight runs of this series proved to be subject to singularities.

The analysis of the results was based on the displays produced by the graphics programme. These displays, together with comments, are presented in Appendix F.

In the determination of the influence of various combinations of displacement constraints and loading element specifications on the outcome, it was again apparent (cf. section 4.341 and 4.342) that the boundary corners of the mesh provided the focal points of error, and that the prime consideration in overcoming the problem was to specify loading elements which contained these nodes. However, it was again not realised that the total avoidance of singularities requires the judicious choice of not only the corner elements, but all the loading elements.

The analysis of the effects of the specification of fixed displacement boundary conditions was confounded by the singular results of all the runs of the series. A complicating factor involved was the substitution into the second four runs of additional strain-displacement equations in the place of the constrained displacements of the first four runs. These extra equations belonged to elements located at the boundary corners, ie. the region of maximum error, and their beneficial effect

served/58..........

served to counter the detrimental effect of the absence of displacement constraints (cf. the results of runs FEM2C1 and FEM2C6 in Appendix F). However, in spite of the above-mentioned problems, the results of run FEM2C2, when compared with those of runs FEM2C6 and FEM2C7, indicated an increase in the errors due to singularity which occurs when fixed-displacement boundary conditions are not specified. The theoretical predictions in regard to this matter (cf. section 2) were thereby considered to be confirmed.

4.344 Data model FEM3. With the obvious exception of the datum run FEM31, all the runs of the series proved to be subject to singularities.

The analysis of the results was based on the displays produced by the graphics programme. These displays, together with comments are presented in Appendix G.

The only result which was explicable in terms of the contemporary theory was that of run FEM39: the absence of all displacement constraints resulted in an obvious case of singularity, in which the reduction processes were halted due to the inability to locate pivots (not even roundoff errors caused effective location of the mesh).

In retrospect of the later theory, it is evident that the singularities which occurred in the runs FEM32 to FEM39 stemmed from the incorrect choice of loading elements. The case least effected by ill-conditioning was that of FEM32, in which the small number of substitutions made with the randomly chosen loading elements minimised the linear dependence and hence singularity effects. In the remainder of the series, it can be seen that the errors were reduced wherever loading elements located near the indeterminate nodes were used.

With reference/59.........

With reference to the objective set for the series (cf. section 4.336), it is evident that, provided that the minimum number of displacement constraints are specified and the choice of loading elements is based on considerations of the linear dependence relationships, the choice of the location of the fixed-displacement boundary conditions is of no significance.

4.345 <u>Conclusions.</u> The results obtained in this phase of the testing were clearly contradictory to the predictions of the contemporary theory. In particular, the apparent limitations in the choice of permissable loading elements were not anticipated by the theoretical model, which allowed for a random choice based on convenience. It was evident therefore that the existing model was in need of revision, based on the conclusions drawn in the analyses of the computer tests. The subsequent reassessment of the theory led to the discovery of the significance of the linear dependence/independence relationships existing between the strain-displacement equations and the force-displacement equations which they replace. This in turn provided the explanation for the previously considered incongruities in the results of the testing.

It should be noted that the original intention of comparing the results obtained in the laboratory testing with those obtained in the computer testing, was thwarted by the presence of the errors due to ill-conditioning in all of the latter results.

4.4 PHASE THREE: TESTING THE REVISED THEORETICAL MODEL ON THE SMALL DATA MODEL

The two objectives set for this phase of the experimental testing may be listed as:

1) the verification of the revised theoretical model;
2) the empirical determination of the relationship between

the singularity phenomenon and the relative locations within the mesh of the loading elements and the indeterminate nodes.

4.41 The Models

The data model FEMS was retained in the form developed for the first phase of testing, and is thus described in section 4.21.

The theoretical model included the aspect of the linear dependence/independence relationships between the strain-displacement equations and the force-displacement equations, thereby incorporating all the theoretical features discussed in chapter 2.

The programme FEMSGT, which was derived from programme FEMSGG, involved no changes to the structure of its predecessor other than the inclusion of a section of coding immediately prior to the reduction of the set of assembly equations. The steps involved in this coding may be summarised as follows:

1) transpose the assembly matrix $[K]$ to form $[K]^T$;
2) transpose the vector representations of all the strain-displacement equations to form $[R]^T$;
3) augment these vectors to $[K]^T$ to form $\left[[K]^T \mid [R]^T\right]$;
4) reduce $\left[[K]^T \mid [R]^T\right]$ to the row-echelon form $\left[[I] \mid [R']\right]$;
5) output the matrix $[R']$.

The output thus obtained enabled the assessment of the linear dependence/independence relationships between the strain-displacement equations and the assembly set of equations.

4.42 The Testing

The testing comprised a set of twenty runs incorporating a sequence of variations in the specification of the loading data. The runs are listed in table H1 of Appendix H.

The first two runs, FEMST1 and FEMST2, were made to verify the revised theoretical model of the method; ie. when the method is used for its intended purpose of providing an alternative to the conventional specification of loading data. The linear dependence relationships between the strain-displacement equations and the force-displacement equation to be replaced (node 2x) were obtained from the conventional analysis of FEMST1, using the coding described in section 4.41. The strain-displacement equation having the strongest linear-dependence relationship was used for the substitution in FEMST2.

The remaining runs of the series contained arbitrary specifications of loading data, in order to examine the effects of the relative locations of the loading elements and the indeterminate nodes on the analysis. These runs cannot thus be considered to be typical of the intended utilisation of the proposed method.

4.43 Analysis of the Results

A programme was written to compare, on a percentage error basis, the results of the various runs in terms of displacements, using FEMST1 as the datum. These comparisons are tabulated in Appendix H.

Run FEMST2 provided conclusive proof of the theory of the proposed method: the attention paid to the aspect of linear dependence relationships led to the exact equivalence of the results of the analyisis to those of the conventional analysis, as predicted in chapter 2. It is significant that the examination of the linear dependence relationships between the various strain-displacement equations and the force-displacement equation to be replaced revealed a variation in the strengths of these relationships. The strain-displacement équation with the weakest of these relationships (of the order of 10 less than that used in FEMST2) was therefore used in FEMST3: small errors were generated which may most probably be attributed to a very mild form of ill-conditioning.

From the/62.........

From the analysis of the linear dependence relationships derived in FEMST1 and the results of runs FEMST2 and FEMST3, it was evident that the strength of the relationship was indirectly proportional to the distance between the physical locations of the loading element and the indeterminate node. This factor was further evidenced by the results of the other runs of the series. However, the singularities which occurred in runs FEMST11, FEMST12, FEMST16, FEMST18, FEMST19, FEMST20 indicated the existence of a limit to the number of substitutions involving remote relative locations which can be made without the appearance of severe effects of ill-conditioning (or singularity). This limit appeared to be in the region of four such substitutions, although the results indicated an inconsistency which could be attributed to the manner in which the relevant linearly dependent subsets were structured (cf. section 2.32).

The effects of the alterations which occur to the linear dependence relationships in the event of substitutions were evident to a far lesser extent in the non-singular runs of the series, where slight shifts in the patterns of the strengths of the relationships occurred. By virtue of the sequential manner in which the loading data of the first nine runs of the series was specified, it was possible to observe these patterns using the FEMSGT coding described in section 4.41. With the exception of run FEMST2, none of the runs utilised the strain-displacement equations exhibiting the optimum linear dependence relationships, hence the errors which resulted in runs that otherwise appeared to be sound (eg. FEMST4). However, the changes in the strengths of the relationships were slight in the cases in which loading elements containing the indeterminate nodes were specified, and it was thus apparent that the adherance to this method of specification would serve to minimise errors as well as to obviate the risk of causing the set of equations to become singular.

The conclusions thus reached at the end of this phase of the testing were that the functioning of the method was entirely in accordance with the theoretical predictions, and that in the absence of the rigorous determination of the linear dependence/independence relationships, the rule to be followed in specifying the loading data is that each indeterminate node should be matched with a strain-displacement equation from an element in the immediate vicinity, with preference being given to elements containing the relevant node.

4.5 PHASE FOUR: TESTING THE REVISED THEORETICAL MODEL ON THE PHYSICAL DATA MODELS

The two objectives set for this phase of the experimental testing may be listed as:

1) the verification of the ability of the proposed method to analyse realistic data models;
2) the assessment of the applicability of the empirically determined rule of section 4.43 (the specification of the loading data) to the analysis of realistic data models.

4.51 The Models

The data models used were FEM2B and FEM2C, retained in the form in which they were developed in phase two of the testing and thus described in section 4.31.

The theoretical model was unchanged from that of phase three. However, programme FEMSGG (with extended storage) did not include the additional coding of FEMSGT, as it was decided to restrict the manner in which the loading data was to be specified to the usage of the rule described in section 4.43 (cf. section 3.32).

4.52 The Testing

The testing was restricted to one set of two runs, as tabulated in Appendix J.

In run/64.........

In run FEM2BR, the strains determined in the laboratory testing of phase two were utilised, with care being taken to match each indeterminate node with a strain-displacement equation from an element in the immediate vicinity (preferance being given to elements containing the pertinent node). The specification of the fixed-displacement boundary conditions to prevent rigid-body motion was arbitrarily made.

The strains resulting from the analysis of FEM2BR were utilised as loading data for FEM2CR, with the matching procedure again being followed and the displacement constraints being arbitrarily specified.

4.53 Analysis of the Results

A programme was written to compare, on a percentage error basis, the results of runs FEM2BR and FEM2CR in terms of the displacements of the vertex nodes of the elements. This comparison is presented in Appendix J.

In view of the findings of the previous phase of testing, it was noted that neither of the runs could be considered to be perfectly accurate, and the discrepancies in the displacement results thus could not be interpreted as absolute values of error.

The largest discrepancies occurred at nodes on or adjacent to the boundary of the mesh, an effect of the ill-conditioning phenomenon previously observed in a more severe from in phase two of the testing. The explanation of this behaviour lay in the apparent moderate weakness of the linear dependence relationships between the force-displacement equations and the strain-displacement equations by which they were replaced: the ill-conditioning was thus centred on these degrees of freedom.

However, it was apparent from the relatively close correspondence

of the/65.........

of the two sets of results that neither run contained singularities. This was of great significance, as it clearly demonstrated the ability of the proposed method to analyse data models of a realistic size. Furthermore, the reasonable accuracy of the results at points located within the interior of the meshes indicated the applicability of the empirical rule (of loading specification) to the analysis of realistically sized meshes: the rule is valid, but the results should be treated with caution.

4.6 A SUMMARY OF THE RESULTS OBTAINED IN THE TESTING OF THE METHOD

The two most important results to emerge from the experimental testing were the conclusive proofs of the ability of the proposed method to analyse realistic stress raiser problems, and of the conformity of the behaviour of the method to the theoretical predictions of chapter 2.

The use of the exact method of determining the linear dependence relationships (cf. the algorithm of section 2.32) was shown to provide precise results totally free of the effects of ill-conditioning. However, it was evident that the distinction between linear dependence and independence is not clear-cut, and that the relationships exist in varying degrees of strength. In view of this fact, it was found necessary to qualify the algorithm to ensure that use is made, wherever possible, of the equations exhibiting the strongest linear dependence relationships.

The empirical rule to be used for the alternative specification of loading data was determined: each indeterminate force-displacement equation must be matched with a strain-displacement equation pertaining to an element in the immediate vicinity of the relevant node, with preference being given to elements containing the node. The application of this rule to the

analysis/66.........

analysis of realistically sized meshes was shown to be feasible, although the system does remain susceptible to slight effects of ill-conditioning and is thus not absolutely reliable.

It should be noted that both of the above methods of loading specification require individual strain-displacement equations (three equations per element) in all but the most trivial cases. This configuration thus takes precedence over the summed form of equation (cf. section 2.22).

The mesh configurations used in the testing were constructed prior to the realisation of the importance and nature of the linear dependence relationships between the strain-displacement equations and the force-displacement equations to be replaced. This created problems with the specification of loading elements related to the relevant indeterminate nodes, and served to unnecessarily weaken linear-dependence relationships (eg. the case of element 58 in mesh FEM2A). Any future usage of the proposed method should therefore involve mesh configurations which cater for the boundary specifications.

CHAPTER 5

CONCLUSION

In attaining the objectives set for the project (cf. section 1.2), an adaption of the displacement method of finite element analysis has been devised and developed: the force-displacement equations of the boundary nodes for which no conventional boundary specifications are possible are replaced, within the set of assembly equations, by selected strain-displacement equations for which the strains can be determined by experimental means. Two techniques for the selection of the equations have been proposed, both based on the necessity for linear dependence relationships between the force-displacement equations and the strain-displacement equations with which they are to be replaced: the first involves an analytical determination (by the computer) of the relevant relationships; the second involves a matching (by the user) of the relevant equations, based on the consideration of their respective physical locations within the mesh.

The proposed method has been programmed for use with second order isoparametric elements. This programming includes a system developed for the handling and reduction of the large, sparse and unsymmetric assembly matrix which is inherent in the method.

Tests have been performed on two-dimensional models which have served to establish the validity of the theory and to determine the general performance characteristics of the method. The accuracy of solution has been shown to be related to the choice of the strain-displacement equations and to be therefore affected by the selection method used. The analytical selection technique enables solutions to be obtained which correspond exactly to those of conventional finite element analysis, whereas the solutions obtained when using the alternative technique contain the adverse effects of mild ill-conditioning. However, the latter method is the more economical in terms of computer usage. The choice of selection technique to be used in the analysis of anything other than a very small mesh (a typical example being a two-dimensional mesh of 160 nodes and 60 elements) thus involves a compromise of either the economy of the computing or the accuracy of the solution.

REFERENCES

1. Zienkiewicz, O.C., "The Finite Element Method in Engineering Science", McGraw-Hill, London (1971), Chps. 1-4,6-9,18-20.

2. Lynn, P.P. and Arya, S.K., "Use of the least squares criterion in the finite element formulation", Int. J. Num. Meth. in Eng., 6, 75-88 (1973).

3. Timoshenko, S.P. and Goodier, J.N., "Theory of Elasticity", 3rd ed., McGraw-Hill, (1970).

4. Zienkiewicz, O.C. and Owen, D.R.J., "Least square-finite element for elasto - static problems. Use of 'reduced' integration", Int. J. Num. Meth. in Eng., 8, 341-358 (1974).

5. Szabo, B.A. and Lee, G.C., "Derivation of stiffness matrices for problems in plane elasticity by Galerkin's method", Int. J. Num. Meth. in Eng., 1, 301-310 (1969).

6. Pian, T.H. and Pin Tong, "Basis of finite element methods for solid continua", Int. J. Num. Meth. in Eng., 1, 3-28 (1969).

7. Pin Tong, "New displacement hybrid finite element models for solid continua", Int. J. Num. Meth. in Eng., 2, 73-83 (1970).

8. Dept. of Civil Engineering, University of Southamption, "Variational Methods in Engineering", (1973).

9. Zienkiewicz, O.C. and Cheung, G.K., "The Finite Element Method in Structural and Continuum Mechanics", McGraw-Hill, New York, (1967).

10. Cook, R.D., "Concepts and Applications of Finite Element Analysis", Wiley, (1974).

11. McNeice, G.M. and Hunnisett, S.F., "Mixed-displacement finite-element analysis with particular application using plane-stress triangles", J. Strain Analysis, 7, 243-252 (1971).

12. Melosh, R.J., "Basis for derivation of matrices for the direct stiffness method", J.A.I.A.A., 1, 1631-1637 (1963).

13. Carroll, W.E. and Barker, R.M., "A theorem for optimum finite-element idealizations", Int. J. Solids Structures, 9, 883-895 (1973).

14. Johnson, M.W. and McLay, R.W., "Convergence of the finite element method in the theory of elasticity", J. Appl. Mech., 35, 274-278 (1968).

15. Szabo, B.A. and Tsai, C., "The quadratic programming approach to the finite element method", Int. J. Num. Meth. in Eng., 5, 375-381 (1973).

16. Noble, B., "Applied Linear Algebra", Prentice-Hall. New Jersey, (1969).

17. Oden, J.T., "A general theory of finite elements", Int. J. Num. Meth. in Eng., 1, 205-221, 247-259 (1969).

18. Strang, G., "Approximation in the finite element method", Numer. Math., 19, 81-98 (1972).

19. Bowie, O.L., Freese, C.E. and Neal, D.M., "Solution of plane problems of elasticity utilizing partitioning concepts", J. Appl. Mech., 767-772 (1973).

20. Dixon, J.R. and Strannigan, J.S., "Determination of energy release rates and stress-intensity factors by the finite-element method", J. Strain Analysis, 7, 125-308 (1973).

21. Pin Tong, Pian, T.H.H. and Lasry, S.J., "A hybrid-element approach to crack problems in plane elasticity", Int. J. Num. Meth. in Eng., 7, 297-308 (1973).

22. Chow, C.L. and Lau, K.J., "Finite element analysis of cracked bodies to determine stress intensity factors ", J. Strain Analysis, 11, 18-25 (1976)

23. Freese, C.E. and Bowie, O.R., "Stress analysis of configurations involving small fillets", J. Strain Analysis, 10, 53-58 (1975).

24. Henshell, R.D. and Shaw, K.G., "Crack tip finite elements are unnecessary", Int. J. Num. Meth. in Eng., 9, 495-507 (1975).

25. Irons, B.M., "Engineering applications of numerical integration in stiffness methods", J.A.I.A.A., 14, 2035-7 (1966).

26. Bond, T.J., Swannell, J.H., Henshell, R.D. and Warburton, G.B., "A comparison of some curved two-dimensional finite elements", J. Strain Analysis, 8, 182-190 (1973).

27. Baxter Brown, J. McD., "Introductory Solid Mechanics", John Wiley & Sons, (1973).

28. Cowper, G.R., "Gaussian quadrative formulas for triangles", Int. J. Num. Meth. in Eng., 8, 405-408 (1974).

29. Hellen, T.K., "Effective quadrative rules for quadratic solid isoparametric finite elements", Int. J. Num. Meth. in Eng., 4, 597-599 (1972).

30. Programmers Reference Manual, "Large scale systems MATH-PACK", Sperry-Univac, UP - 7542 rev. 1.

31. Irons, B.M., "A frontal solution program for finite element analysis", Int. J. Num. Meth. in Eng., 2, 5-32 (1970).

32. Hood, P., "Frontal solution program for unsymmetric matrices", Int. J. Num. Meth. in Eng., 10, 379-399 (1976).

APPENDIX A

THE DISPLACEMENT METHOD OF FINITE ELEMENT ANALYSIS - AN EXPLICIT APPROACH WITH GLOBAL, CARTESIAN COORDINATES.

The material presented here is drawn from references 1 and 10.

Considering an element within the finite element mesh.

The displacement functions within an element can be expressed in terms of polynomials of position coordinates, ie. the displacement function

$$\{f\} = \begin{Bmatrix} u(x,y,z) \\ v(x,y,z) \\ w(x,y,z) \end{Bmatrix} \qquad \text{.... (i)}$$

where u, v, and w are the displacements in the x,y, and z directions respectively.
The polynomials are of the form (eg.)

$$u = \alpha_1 + \alpha_2 x + \alpha_3 y + \alpha_4 z + \alpha_5 xy + \quad \text{... etc.}$$

It is evident that the higher the order of the polynomial, the closer will be the approximation of u to the true value. As a limitation must be placed on the polynomial order for reasons of economy and utility, various "families" of elements exist, each characterised by an order of polynomial.
In order to evaluate the polynomials appearing in the element, the same number of nodal points as unknowns α are required, these being placed on the boundaries of the element and, depending on the order of polynomial, in the interior as well.

The unknowns α are solved for by substituting the nodal coordinates and their respective nodal displacements into the displacement function. Thus, for element e,

$$\{\delta\} = [H]\{\alpha\}$$

$$\Rightarrow \{\alpha\} = [H]^{-1}\{\delta\}^e \qquad \text{.... (ii)}$$

where $\{\alpha\}$ is the vector of unknowns

$[H]$ is the matrix (square) containing relevant coordinates

$\{\delta\}^e$ is the vector of respective nodal displacements $\begin{Bmatrix} \delta_i \\ \delta_j \\ \delta_m \\ \vdots \end{Bmatrix}$

where/A-2..........

where $\{\delta_i\} = \begin{Bmatrix} u_i \\ v_i \\ w_i \end{Bmatrix}$ at node i

Equation (i) can be rewritten in its vector form. Using only the polynomial for one displacement it is evident that displacement

$$\phi = [P'] \{\alpha'\}$$
$$= [P'] [H']^{-1} \{\delta'\}^e$$

where the dashed symbols represent those values pertaining to the relevant single polynomial, eg.

$u = [P']\{\alpha'\}$ ... where $[P']$ contains the generalised position coordinates.

In general then $\{f\} = [P]\{\alpha\}$

$$= [P] [H]^{-1} \{\delta\}^e \qquad \text{.... (iii)}$$

Writing $[N] = [P] [H]^{-1}$ where $[N]$ is known as the shape function, it can be seen that

$$\{f\} = [N]\{\delta\}^e$$
$$= [N_i, N_j, N_m, \ldots] \begin{Bmatrix} \delta_i \\ \delta_j \\ \delta_m \\ \vdots \end{Bmatrix} \qquad \text{.... (iv)}$$

Strains are of the form

$$\{\varepsilon\} = \begin{Bmatrix} \varepsilon_x \\ \varepsilon_y \\ \varepsilon_z \\ \gamma_{xy} \\ \gamma_{yz} \\ \gamma_{zx} \end{Bmatrix} = \begin{Bmatrix} \frac{\partial u}{\partial x} \\ \frac{\partial v}{\partial y} \\ \frac{\partial w}{\partial z} \\ \frac{\partial u}{\partial y} + \frac{\partial v}{\partial x} \\ \frac{\partial v}{\partial z} + \frac{\partial w}{\partial y} \\ \frac{\partial w}{\partial x} + \frac{\partial u}{\partial z} \end{Bmatrix} \qquad \text{.... (v)}$$

Differentiating the displacements in $\{f\}$ with respect to these conditions results in $\{\varepsilon\} = [B]\{\delta\}^e = [B_i, B_j, B_m, \ldots\ldots]\{\delta\}^e$

.... (vi)

where

$$[B_i] = \begin{bmatrix} \frac{\partial N_i}{\partial x} & 0 & 0 & \frac{\partial N_i}{\partial y} & 0 & \frac{\partial N_i}{\partial z} \\ 0 & \frac{\partial N_i}{\partial y} & 0 & \frac{\partial N_i}{\partial x} & \frac{\partial N_i}{\partial z} & 0 \\ 0 & 0 & \frac{\partial N_i}{\partial z} & 0 & \frac{\partial N_i}{\partial y} & \frac{\partial N_i}{\partial x} \end{bmatrix}^T$$

.... (vii)

It is evident that such a matrix can be easily evaluated.

The stresses can be obtained by using the correct stress/strain relationship $[D]$, where $[D]$ is a matrix containing the relevant elastic constants. Ignoring initial stresses and strains we

thus/A-3.........

thus have

$$\{\sigma\} = [D]\{\varepsilon\}$$
$$= [D]\ [B]\{\delta\}^e \qquad \text{.... (viii)}$$

The nodal forces which are statically equivalent to the boundary stresses and distributed loads on the element can be expressed as

$$\{F\} = \begin{Bmatrix} F_i \\ F_j \\ F_m \\ \vdots \end{Bmatrix}$$

To establish the overall conditions of equilibrium of the element the Principle of Virtual Work is used. A set of virtual displacements is imposed, and if the virtual work due to the external forces is equal to the virtual strain energy, the element is in equilibrium. Thus by equating these two factors:

$$\{F\}^e = \left(\int_V [B]^T\ [D]\ \ [B]\ dV \right) \{\delta\}^e \qquad \text{.... (ix)}$$

or, to abbreviate this

$\{F\}^e = [K']^e\{\delta\}^e$ where $[K']^e$ is known as the element stiffness matrix. .... (x)

Alternatively, the nodal force equivalent to the element strain energy function can be written as

$$F_{i;e} = K'_{ii;e}\delta_i + K'_{ij;e}\delta_j + K'_{im;e}\delta_m + \ldots\ldots$$
$$\text{.... (xi)}$$

Considering the body as a whole

The derivation above applies to the individual element. However, the assembly stiffness equations can be deduced by application of the twin conditions of compatability of displacement and equilibrium at the nodes.

The first condition has been satisfied by the use of nodal displacements to define element behaviour. These displacements are related to nodal coordinates expressed in global terms. Since elements share nodes on common boundaries, inter-element

compatibility/A-4.........

compatibility must exist.

The second condition requires that at any node q the external load F_q must be the resultant of the loads exerted on/by the elements meeting at that node, ie.

$$F_q = \sum_{e=1}^{n} F_{q;e} \qquad \text{.... (xii)}$$

where n is the number of nodes in the whole body: those elements not having a node at q making zero contribution. Combining equations (ix) and (x) it is seen that

$$F_q = K_{q1}\delta_1 + K_{q2}\delta_2 + \ldots\ldots K_{qp}\delta_p + K'_{qr}\delta_r \qquad \text{.... (xiii)}$$

where r is the total number of nodes, and

$$[K_{qp}] = \sum_{e=1}^{n} K'_{qp;e}$$

Taking all nodes into account by extending eqn.(xiii) to cover all nodes, the assembly equations are arrived at:

$$\{F\} = [K]\{\delta\} \qquad \text{.... (xiv)}$$

where $\{F\}$ is the vector of nodal forces

$[K]$ is the assembly stiffness matrix

$\{\delta\}$ is the vector of nodal displacements

APPENDIX B

THE PHASE ONE TESTING OF MODEL FEMS

This appendix is related to section 4.2 of the report. The model FEMS is illustrated here for the sake of convenience.

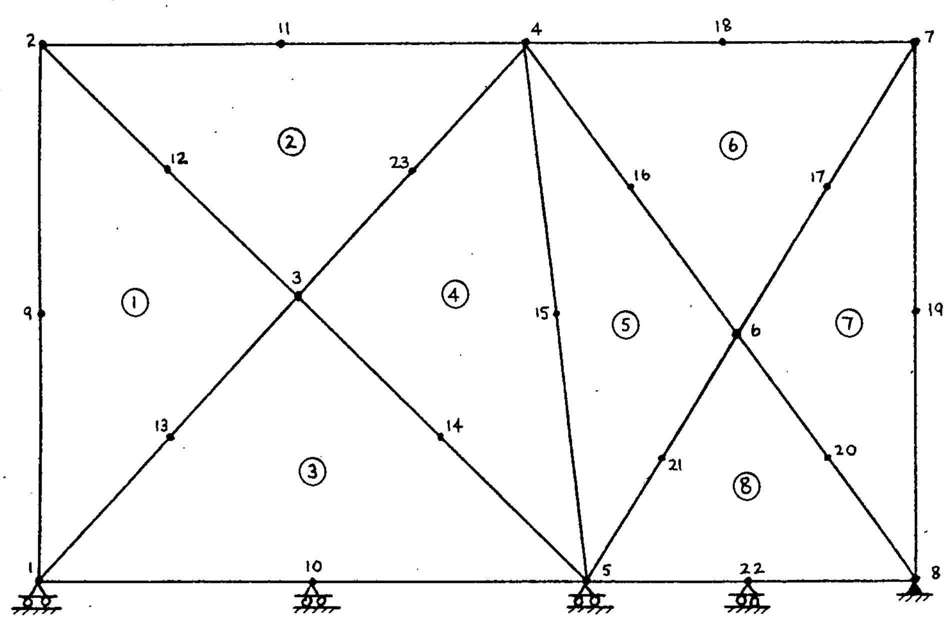

Figure B1. Mesh FEMS (the element numbers are ringed.)

The characteristics of the runs made in the first phase of testing are listed in table B1. All displacement boundary conditions are taken as free (ie. force specified as zero) unless otherwise stated. The x and y subscripts refer to the Cartesian coordinate components of the relevant identities.

RUN	DISPLACEMENT BOUNDARY CONDITIONS		LOADING	
	fixed nodes	indeterminate nodes	nodal forces	element strains
FEMS1	1y,5y,8xy,10y,22y	none	2x	none
FEMS2	ditto	2xy,7xy,9xy	none	1,5
FEMS3	1xy,9x	5y,8xy,10y,22y	2x	3,8
FEMS4	none	1y,5y,8xy,10y,22y	2x	3,8
FEMS5	none	1y,2x,5y,8xy,10y,22y	none	2,3,8
FEMS6	none	none	2x	none

Table B1. The Characteristics of the Phase One Series on FEMS

In table B2 the displacements of the vertex nodes, computed in the runs, are expressed as percentage errors of the corresponding displacement values of run FEMS1. The asterisks indicate values in exess of 10000%.

NODES	FEMS2	FEMS3	FEMS4	FEMS5	FEMS6
1x	.02074	-100.00000	126.23230	392.11813	*******
1y	.00000	.00000	-.00002	.00002	.34411
2x	-.05359	-56.87805	-269.92089	409.32370	*******
2y	-.03373	.00071	-925.97086	964.60899	*******
3x	-.00255	-105.17102	-255.05739	623.81828	*******
3y	1.02903	1694.74551	*******	*******	*******
4x	.02279	-108.25890	-513.75890	779.09460	*******
4y	.11678	734.02361	3529.41675	716.80846	*******
5x	-.01937	-143.62665	181.30121	563.17641	*******
5y	.00000	.00000	.00001	-.00000	-1.05729
6x	-.00743	-130.32756	-236.60265	729.71173	*******
6y	-2.50012	9505.19214	*******	*******	*******
7x	.13146	-119.81000	-568.57443	862.22767	*******
7y	1.45077	-583.05389	*******	3359.06863	*******
8x	.00000	-.00000	.00000	.00001	.08801
8y	.00000	.00000	.00002	-.00001	-.23290

Table B2. The Errors in Displacements Computed as Percentages

It should be noted that the values for nodes 1y,5y,8xy are erroneously computed. The zero displacement at these nodes in run FEMS1 should have resulted in infinite percentage errors, but floating-point overflow has produced actual values.

In table B3 the σ_x, computed for the vertex nodes in the runs, are expressed as percentage errors of the corresponding σ_x value of FEMS1.

NODES	FEMS2	FEMS3	FEMS4	FEMS5	FEMS6
1	-.18710	.00028	.00074	-.00459	31.04921
2	-.11092	-.00071	.00002	-.00104	1.91518
3	.00299	-.03073	.00328	-.00443	21.14120
4	-.60245	-.01075	.00161	-.02176	156.68621
5	.09266	.00704	-.00129	-.01331	-132.78050
6	-6.01144	.80417	-.19746	-5.90998	-214.50860
7	.59505	.00506	-.00039	-.07950	-132.64461
8	.00431	.00497	-.00187	-.08901	-100.49726

Table B3. The Stresses σ_x Computed as Percentage Errors

APPENDIX C

COMPUTER GRAPHICS OF THE MESHES AND OF THE EXPERIMENTAL STRESSES

Two graphics programmes written by Mr. J.E. Newmarch were used to display computer data involved in the project, namely:

1) DATACHECK: a programme to aid the checking of the input data for finite element programmes by providing plots of the meshes together with the node and element numbers;
2) STRESSPLOT: a programme to display, within the outline of the mesh, the principal stress vectors computed at the element vertex nodes by the relevant finite element programme.

Both programmes contain "window-changing" facilities, and STRESSPLOT also provides for the alteration of stress vector scaling.

This appendix contains reproductions of the displays output by DATACHECK when used on the meshes of the project, and by STRESSPLOT when used to check the data obtained by experimental means (laboratory testing) for models FEM1 and FEM2. In the latter case the conventional programme was modified to plot the principal stress vectors at the relevant element centroids so as to correspond with the locations of the strain measurements.

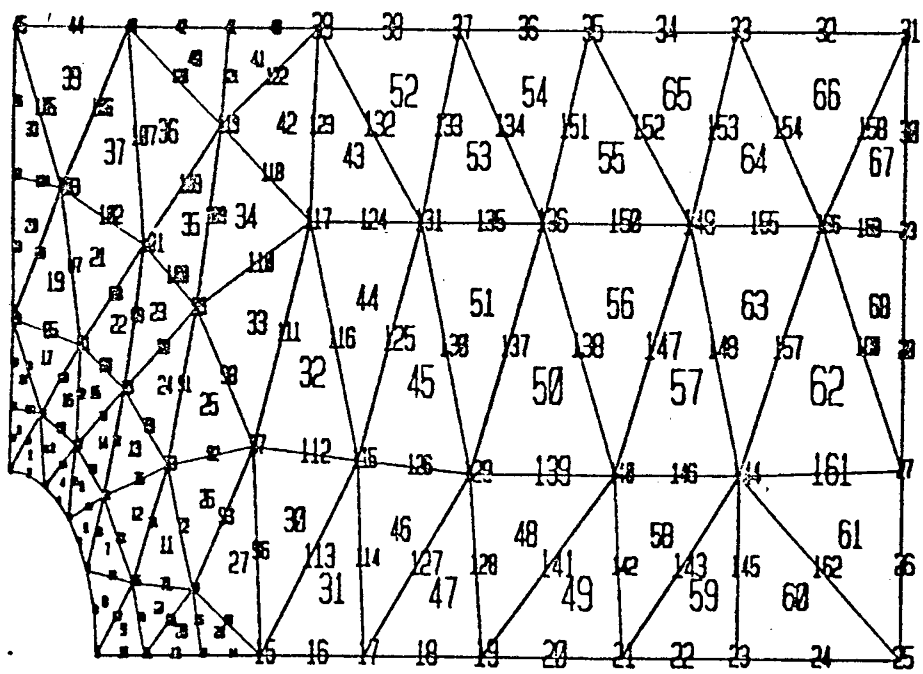

Figure C1. The Mesh FEM1

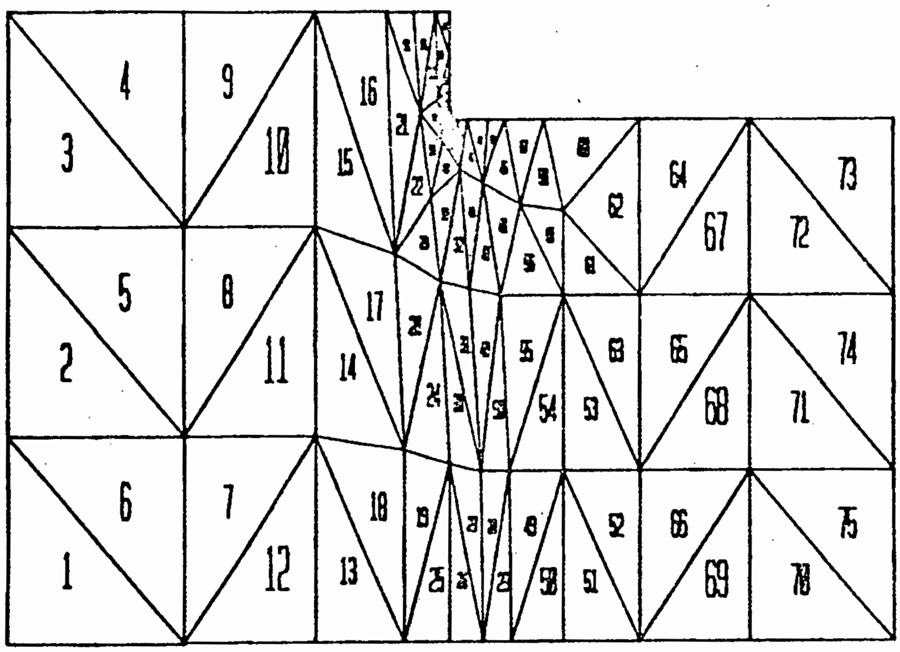

Figure C2. The Mesh FEM2

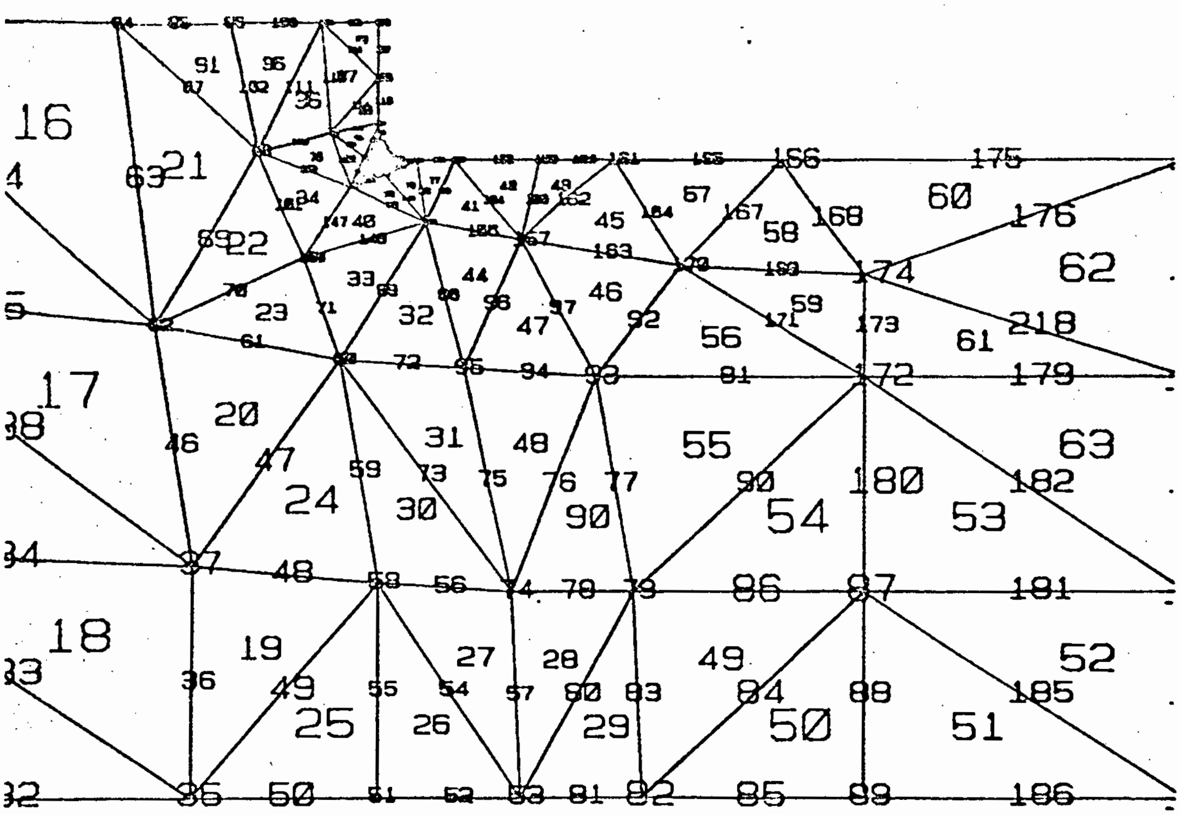

Figure C3. A Detail of the Central Portion of Mesh FEM2.

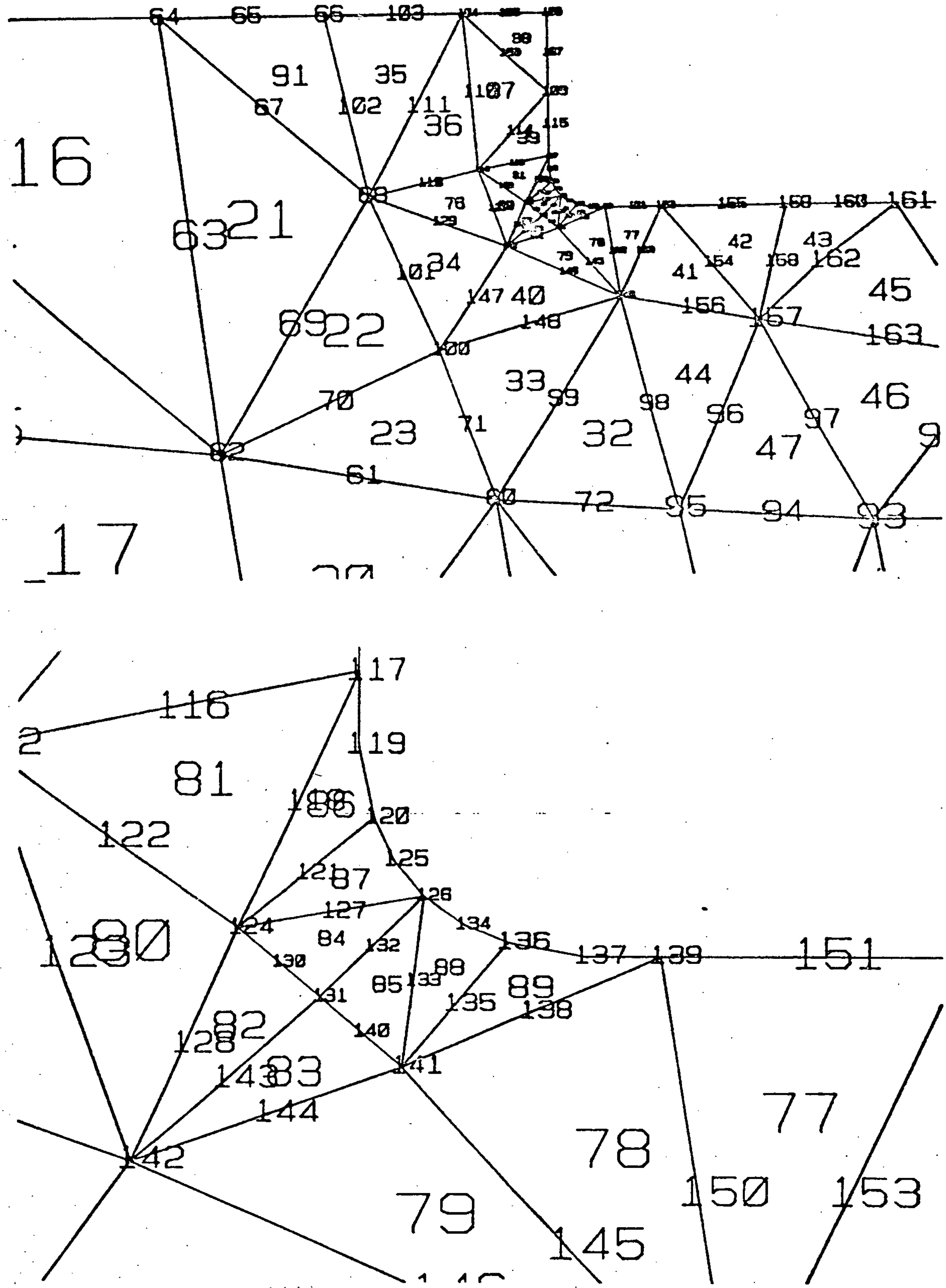

Figure C4. Details of the Mesh Surrounding the Fillet in Model FEM2. The node number shown is that of mesh FEM2, but the mesh configuration is constant for the FEM2 series.

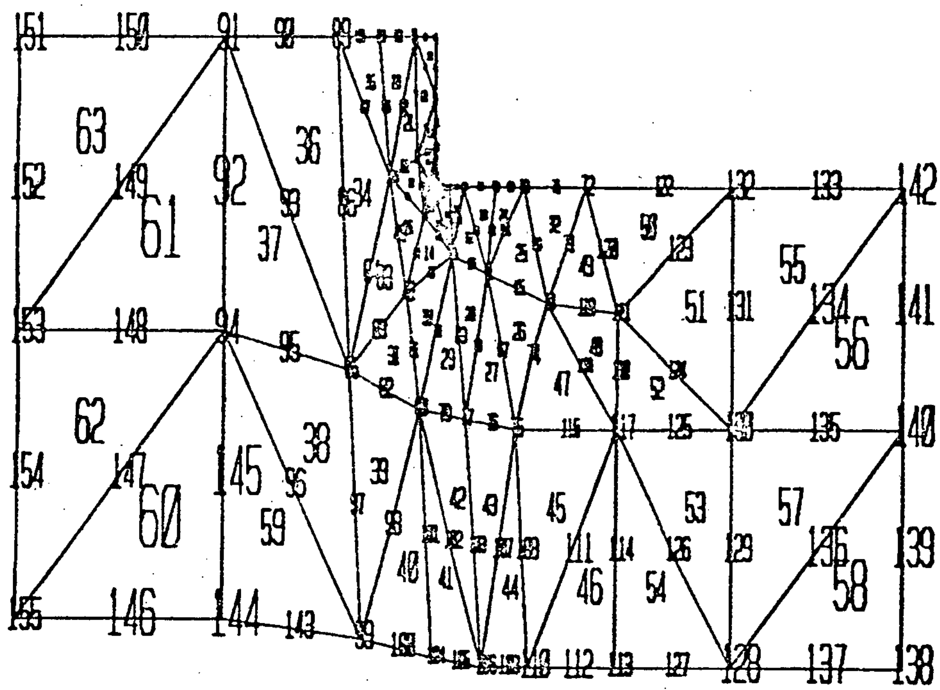

Figure C5. The Mesh FEM2A

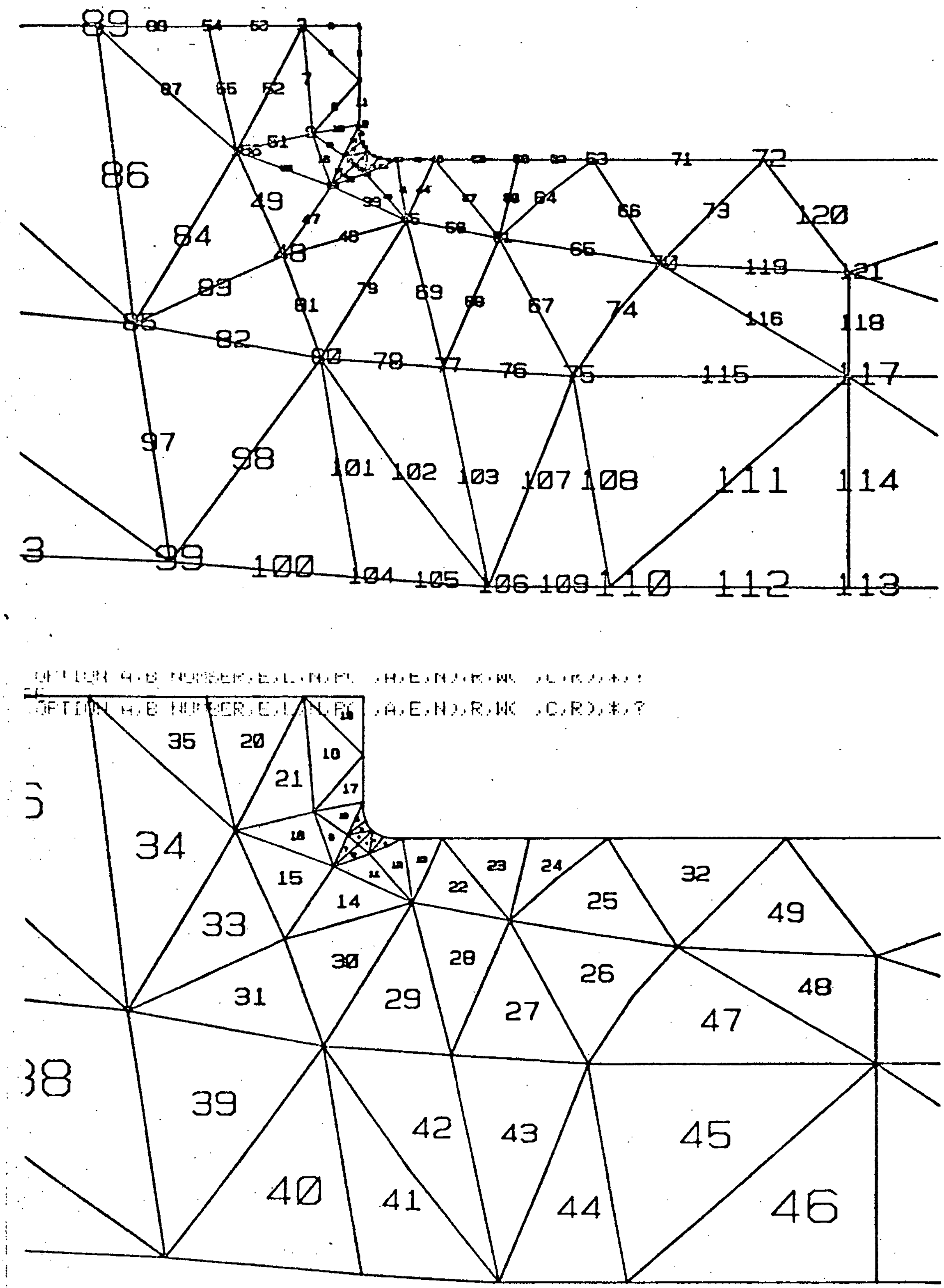

Figure C6. Details of the Central Portion of Mesh FEM2A Showing the Node and Element Numbering Individually

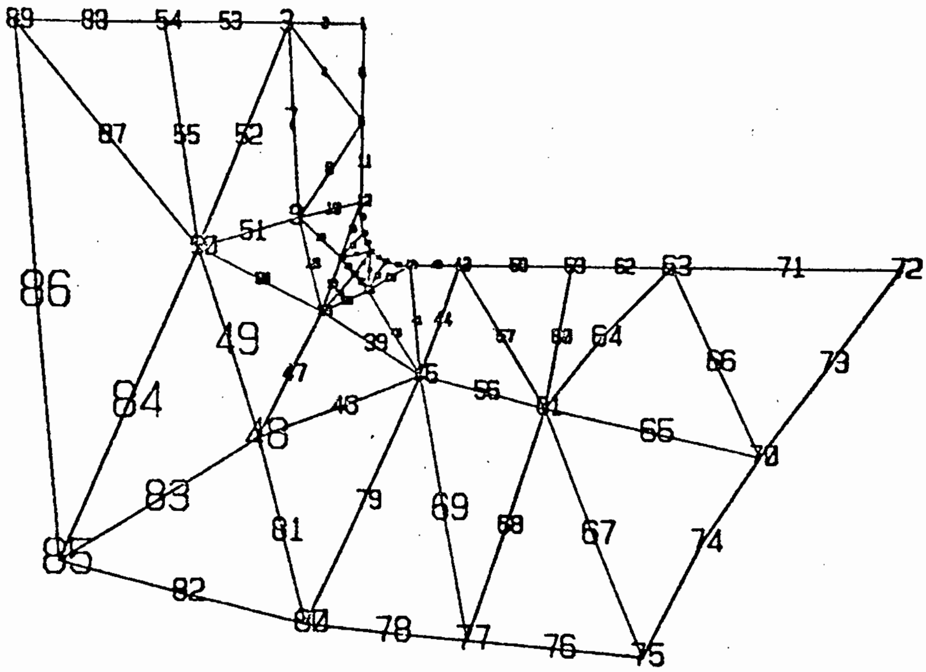

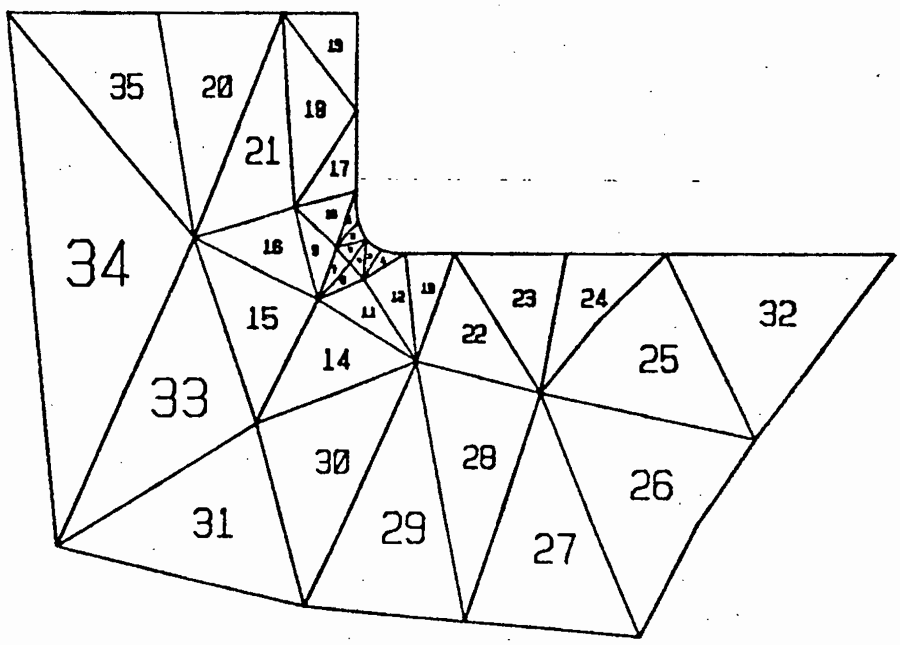

Figure C7. The Mesh FEM2B, Showing the Node and Element Numbering Individually

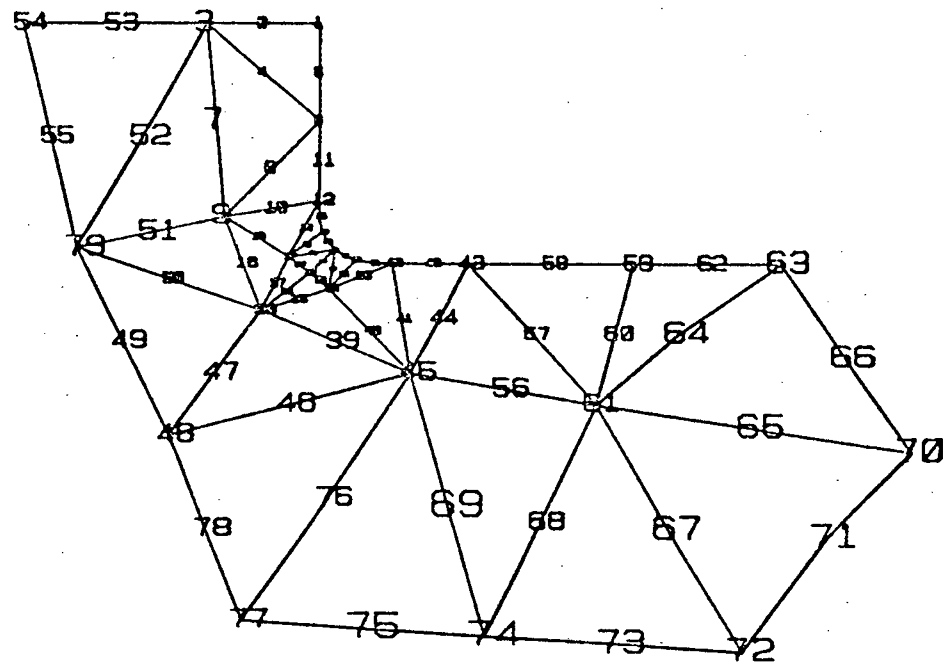

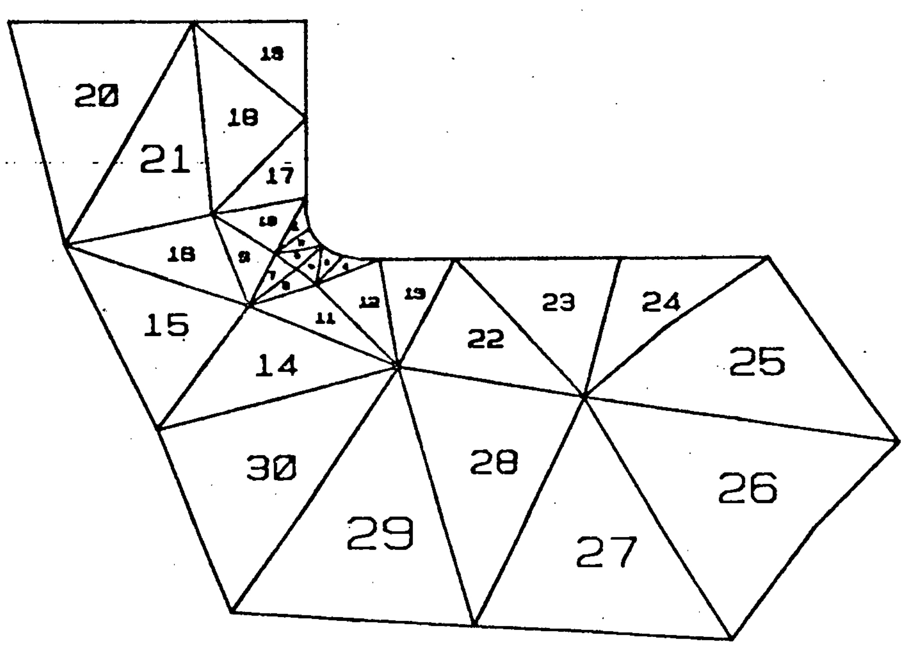

Figure C8. The Mesh FEM2C, Showing the Node and Element Numbering Individually

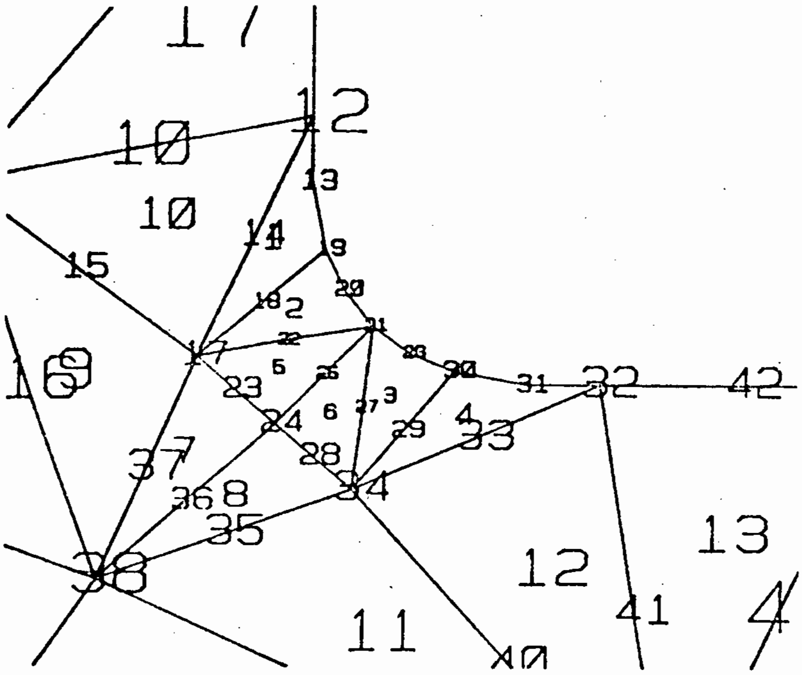

Figure C9. A Detail of the Mesh Surrounding the Fillet in Meshes FEM2A, FEM2B, FEM2C

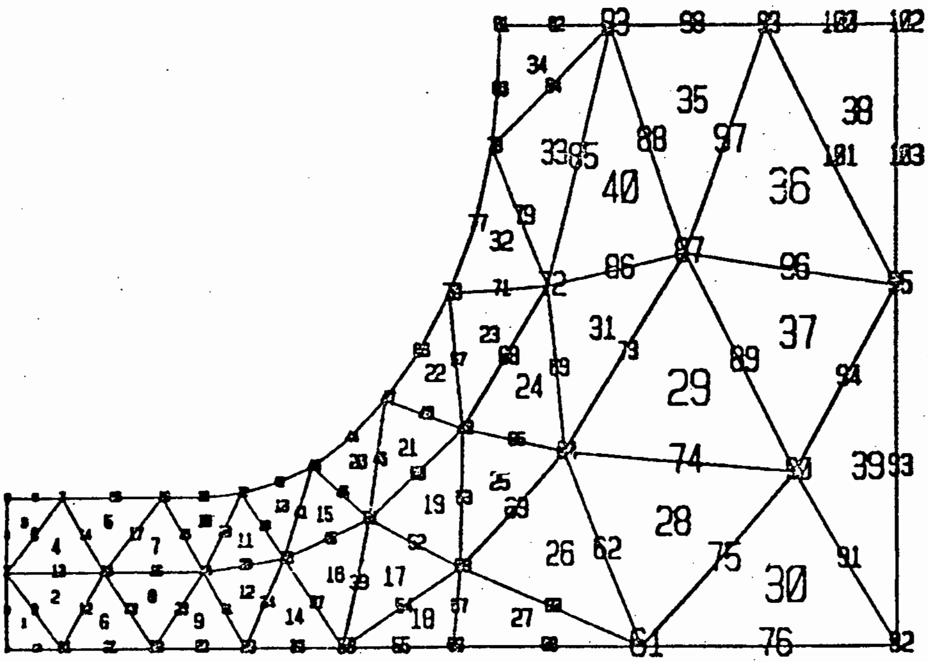

Figure C10. The Mesh FEM3

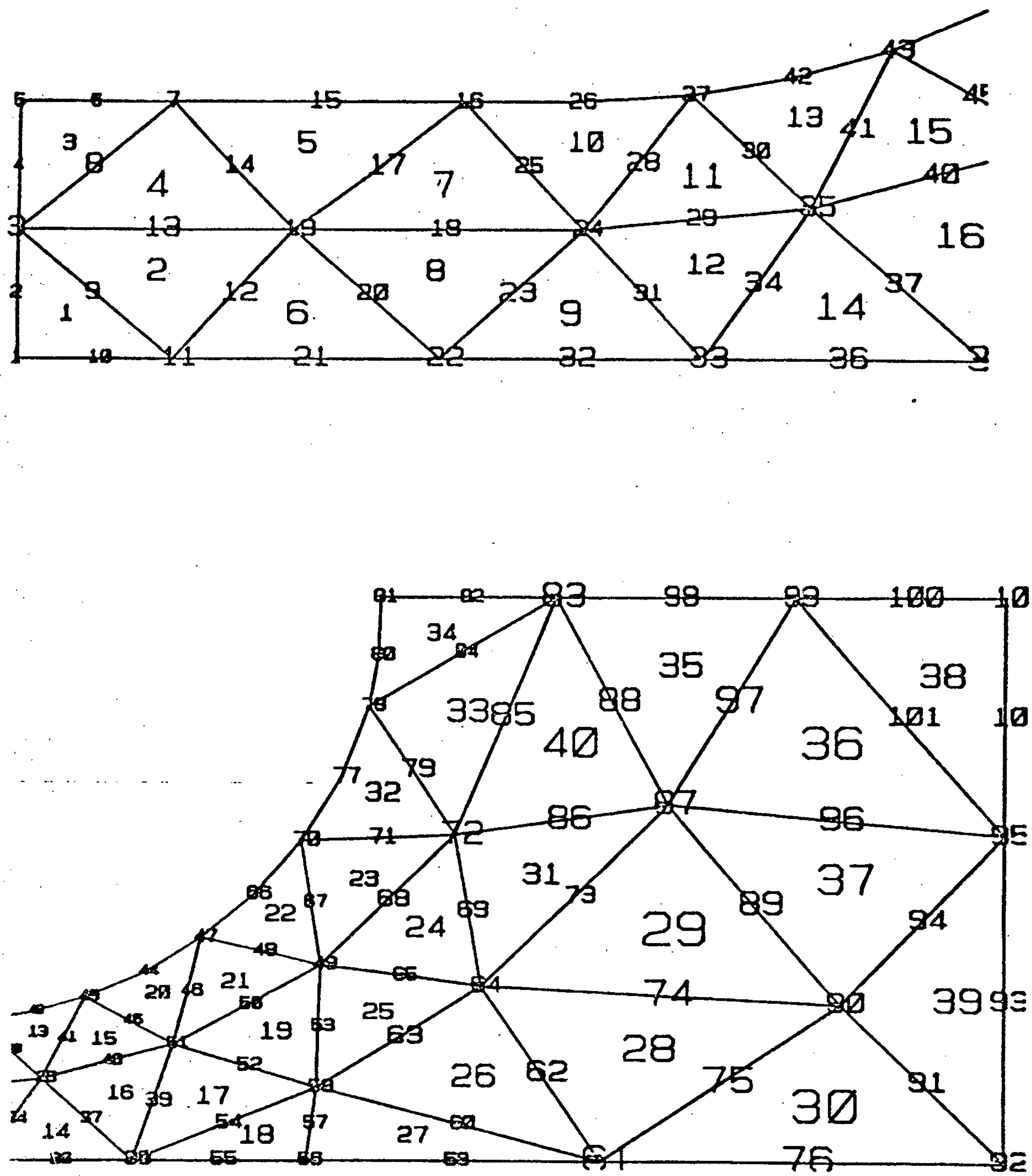

Figure C11. Details of the Mesh FEM3

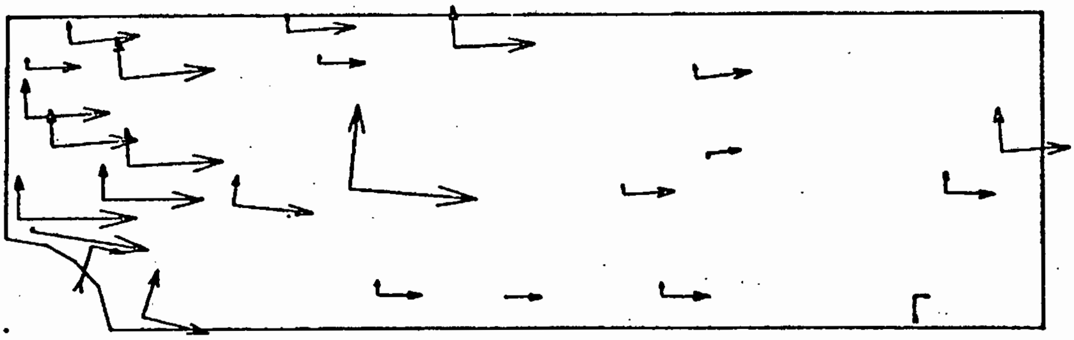

Figure C12. The Principal Stress Vectors (plotted at the element centroids) for the Experimentally Determined Values of Model FEM1

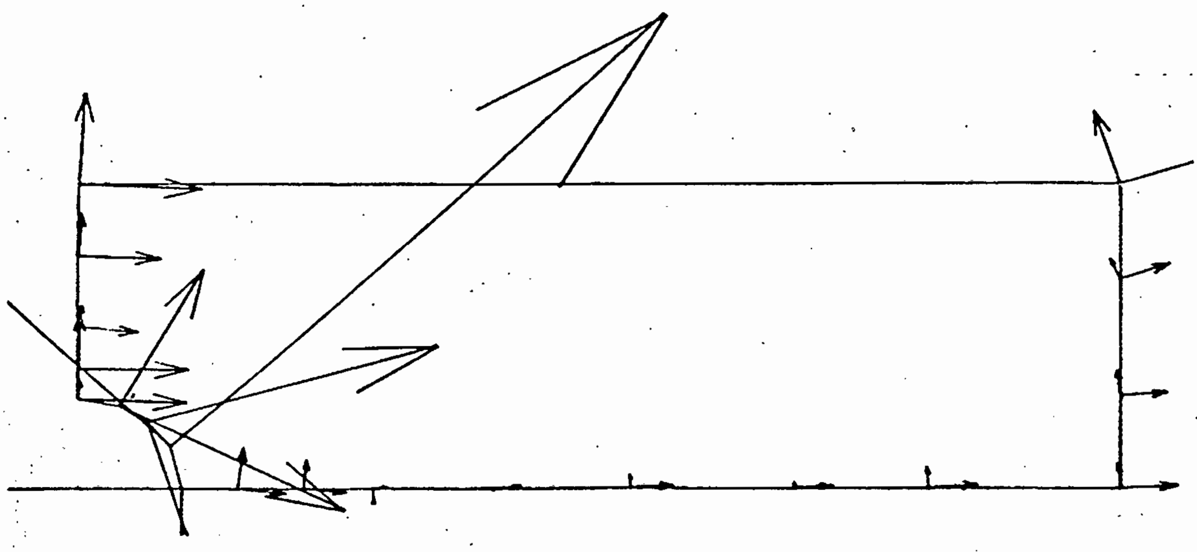

Figure C13. The Principal Stress Vectors (plotted at the element vertrices) for the Experimentally Determined Values of Model FEM1

APPENDIX D

THE PHASE TWO TESTING OF MODEL FEM2A

This appendix is related to sections 4.333 and 4.341 of the report. The reader is referred to Appendix C for the illustrations of the mesh.

The characteristics of the runs made in the series are listed in table D1.

RUN	DISPLACEMENT BOUNDARY CONDITIONS		LOADING
	fixed nodes	indeterminate nodes	elements
FEM2A1	138x,155xy	remaining internal bds.	14,15,16,22
FEM2A2	138x,(151 - 155)xy	ditto	23,24,25,28
FEM2A3	138x,(151 - 155)x	ditto	29,30,31,32
FEM2A4	none	internal boundaries	33,34,35,38

Table D1. The Characteristics of the Runs

APPENDIX E

THE PHASE TWO TESTING OF MODEL FEM2B

This appendix is related to sections 4.334 and 4.342 of the report. The reader is referred to Appendix C for illustrations of the mesh.

The characteristics of the runs made in the series are listed in table E1.

RUN	DISPLACEMENT BOUNDARY CONDITIONS		LOADING
	fixed nodes	indeterminate nodes	elements
FEM2B1	76y,80xy	remaining internal bds.	14,25,26,27, 28,29,31
FEM2B2	none	internal boundaries	14,15,22,23, 24,25,28,29
FEM2B3	none	ditto	14,25,28,29, 31,32,33,34
FEM2B4	none	ditto	14,25,26,28, 29,31,32,33,34
FEM2B5	none	ditto	14,25,26,27, 28,29,31,32

Table E1. The Characteristics of the Runs

All five runs were processed using the graphics programme STRESS-PLOT, and copies are presented in the following pages of the appendix.

It should be noted at this juncture that STRESSPLOT scales the plotting of the vectors according to the maximum value present.

The diagonal line drawn in the upper left-hand part of the mesh boundary is an unavoidable inclusion in the plot and should be ignored in all the plots in this and the FEM2C series.

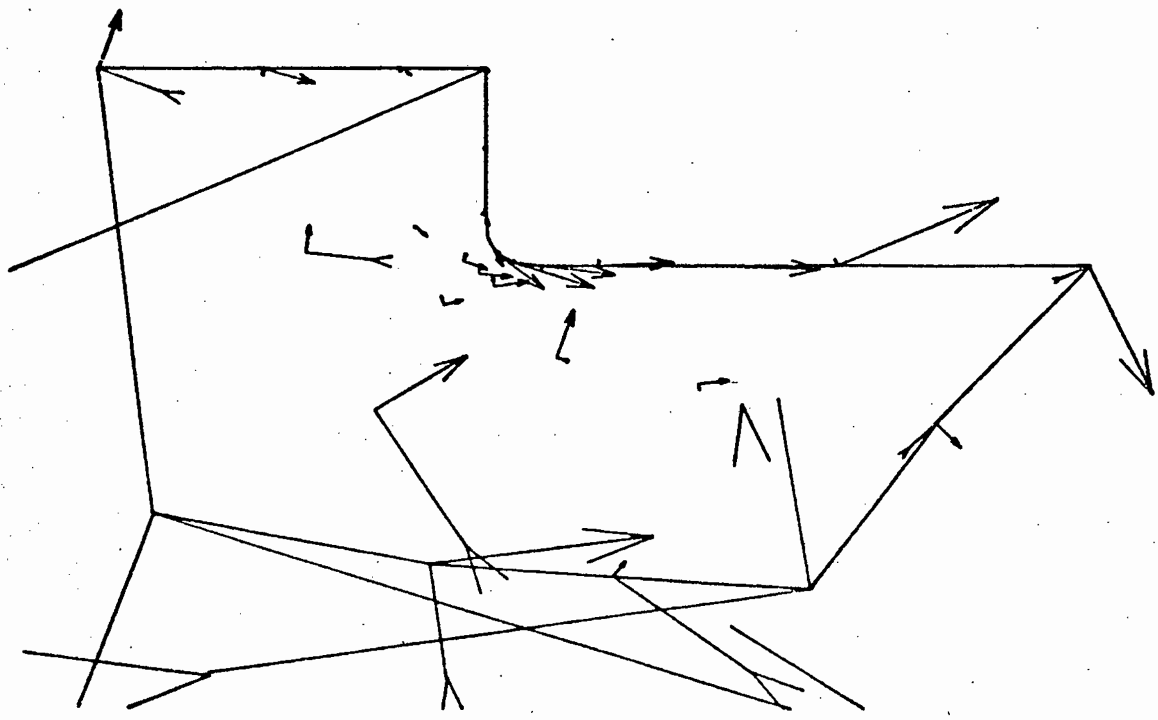

Figure E1. The Principal Stress Vectors of FEM2B1. The erratic stress values at the boundaries are clearly evident, with the worst cases being at corner nodes 75 and 85. The region surrounding the fillet is relatively well-conditioned.

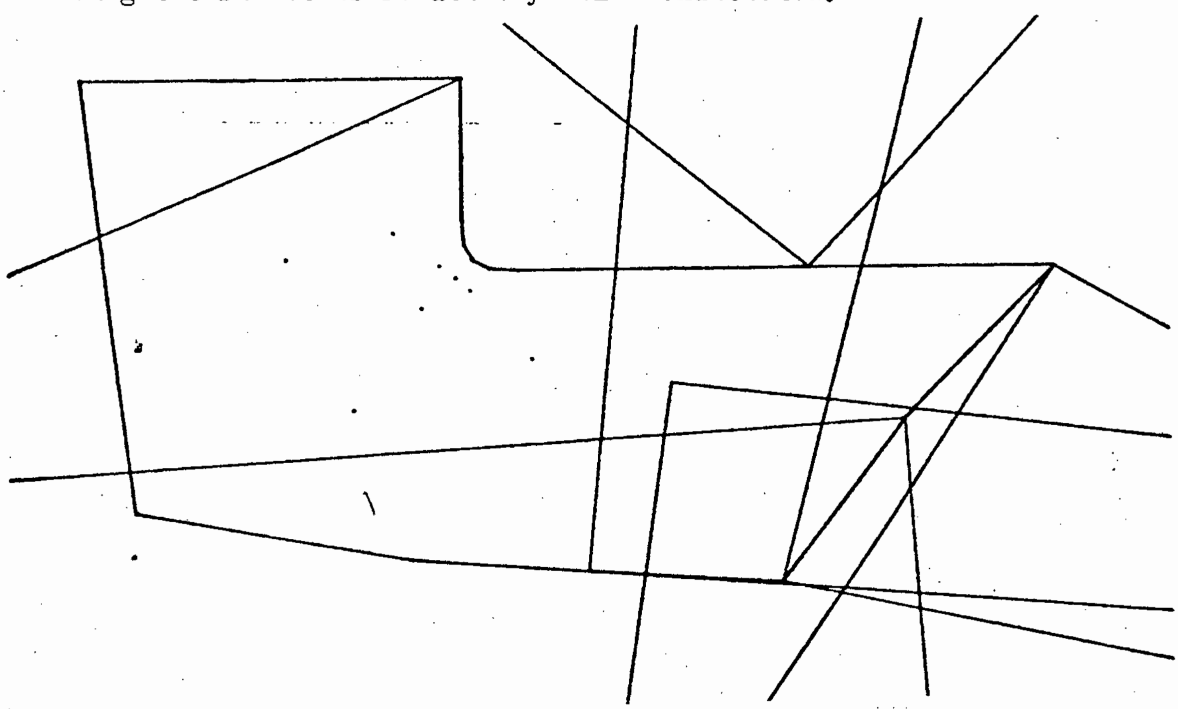

Figure E2. The Principal Stress Vectors of FEM2B2. This plot demonstrates the severe ill-conditioning that occurs when the majority of the loading elements chosen are not located along the mesh boundary.

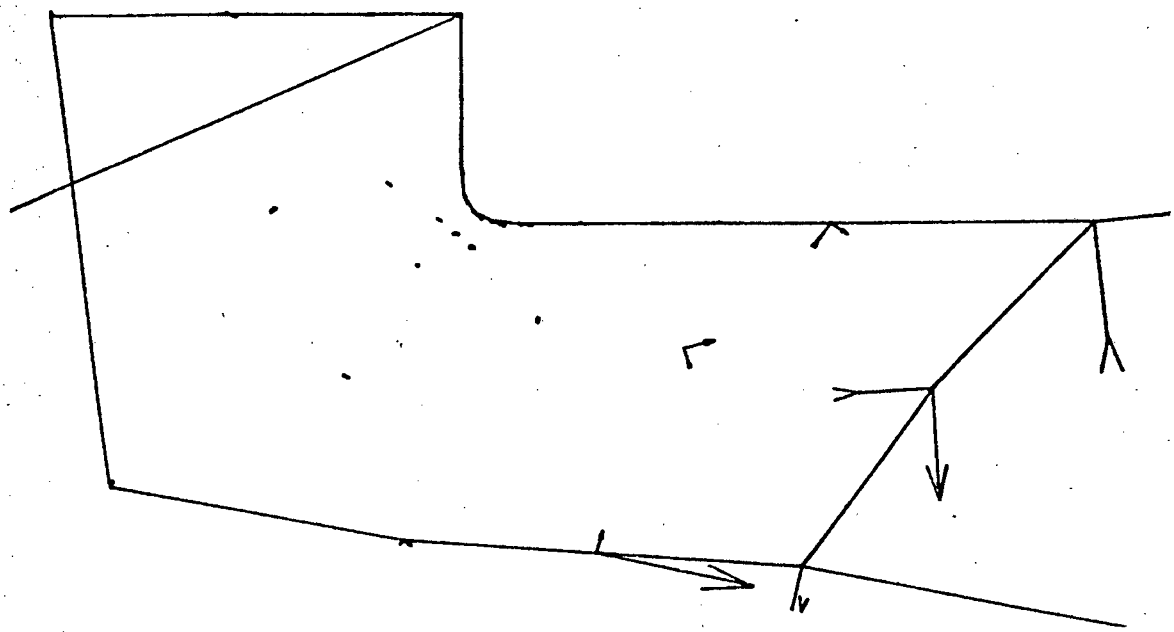

Figure E3. The Principal Stress Vectors of FEM2B3. The concentration of the ill-conditioning effects in the lower right-hand corner of the mesh is a result of failure to specify loading elements in the region (elements 26 and 27).

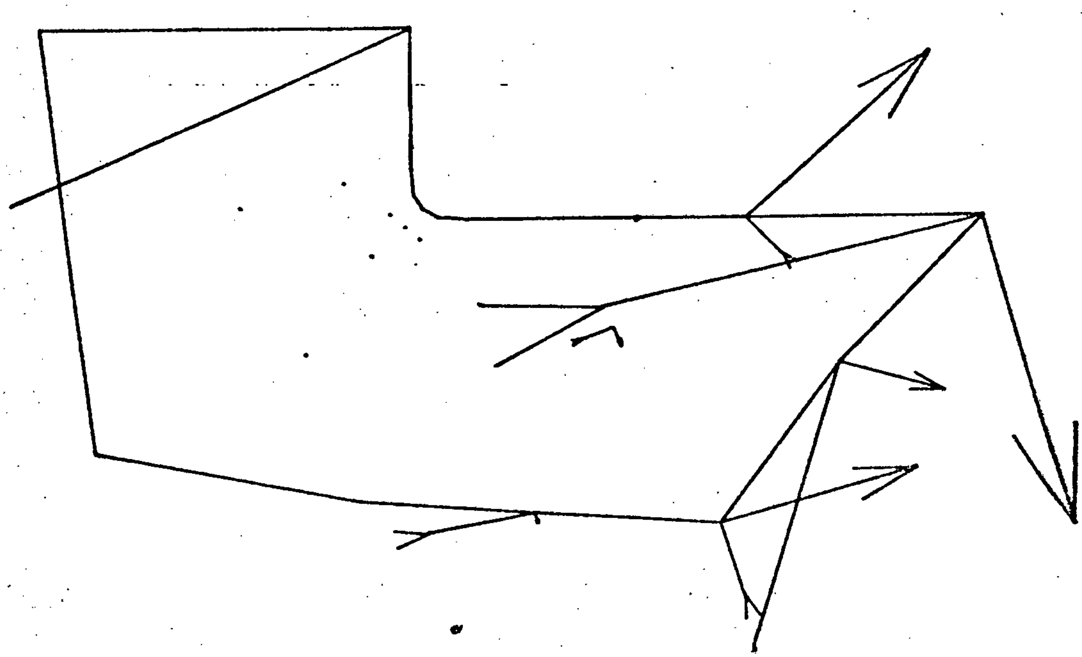

Figure E4. The Principal Stress Vectors of FEM2B4. The ill-conditioning effects located at the right-hand side of the mesh can be attributed to the failure to specify element 27 as a loading element.

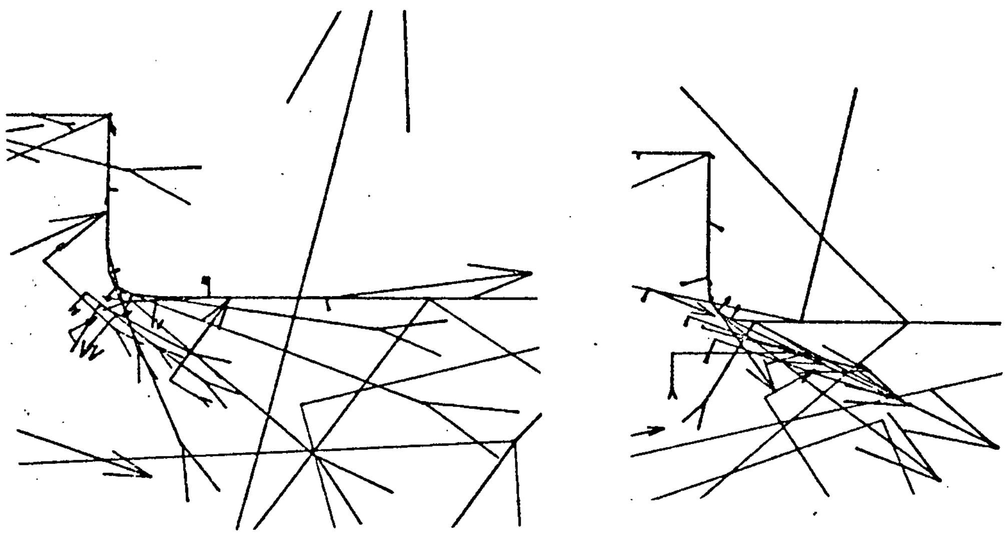

Figure E5. The Principal Stress Vectors of FEM2B3 and FEM2B4. This scaled-up plot of (a) FEM2B3 and (b) FEM2B4 indicates the vast improvement of the latter run in producing tensile stresses in the fillet, compared to the compressive stresses of the former run. The improvement gained in specifying a loading element in the bottom right-hand corner is thus evident.

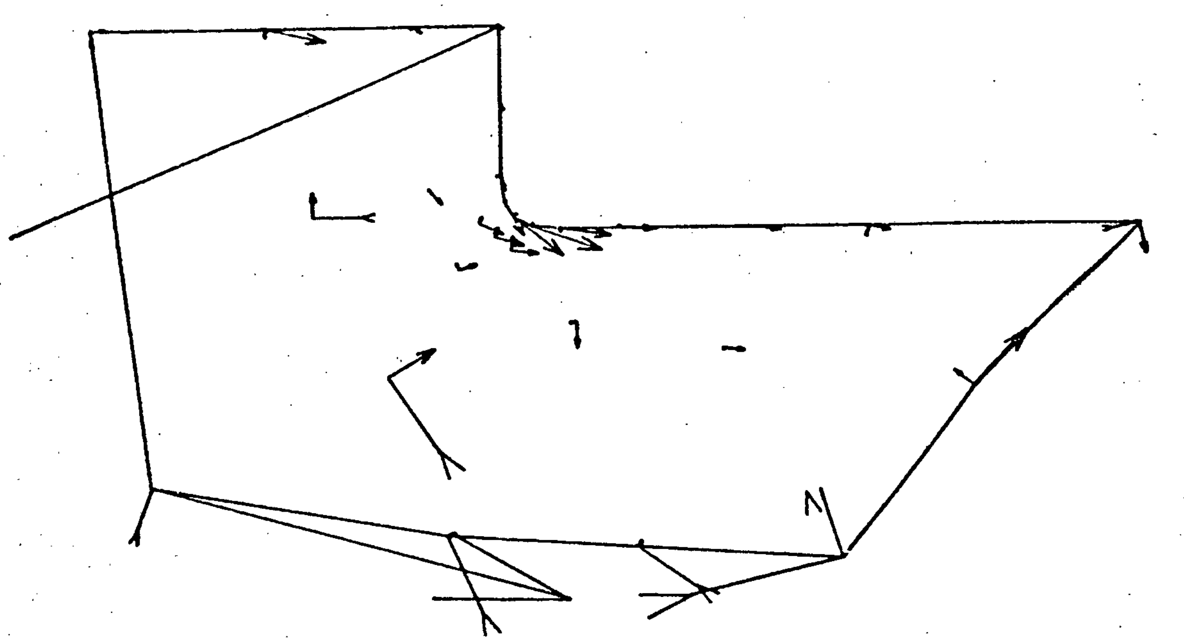

Figure E6. The Principal Stress Vectors of FEM2B5. The ill-conditioning effects located at the left-hand side of the mesh can be attributed to the failure to specify loading elements in the region (elements 33 and 34).

APPENDIX F

THE PHASE TWO TESTING OF MODEL FEM2C

This appendix is related to sections 4.335 and 4.343 of the report. The reader is referred to Appendix C for illustrations of the mesh.

The characteristics of the runs made in the series are listed in table F1.

RUN	DISPLACEMENT BOUNDARY CONDITIONS		LOADING
	fixed nodes	indeterminate nodes	elements
FEM2C1	72x,77xy	remaining internal bds.	14,15,16,22,23, 24,25,26,27,28
FEM2C2	ditto	ditto	15,16,20,24,25, 26,27,28,29,30
FEM2C3	70xy,72xy,77xy	ditto	15,16,20,24,25, 26,27,28
FEM2C4	70xy,72xy	ditto except for 77	ditto
FEM2C5	none	internal boundaries	14,15,16,22,23, 24,25,28,29,30
FEM2C6	none	ditto	14,15,16,22,23, 24,25,26,27,28
FEM2C7	none	ditto	15,16,20,24,25, 26,27,28,29,30
FEM2C8	none	ditto except for 54y,63y	ditto

Table F1. The Characteristics of the Runs

The results of the runs made in this series are best depicted in graphical form, and copies taken from the graphics programme STRESSPLOT are presented for all runs excepting the nearly singular FEM2C5.

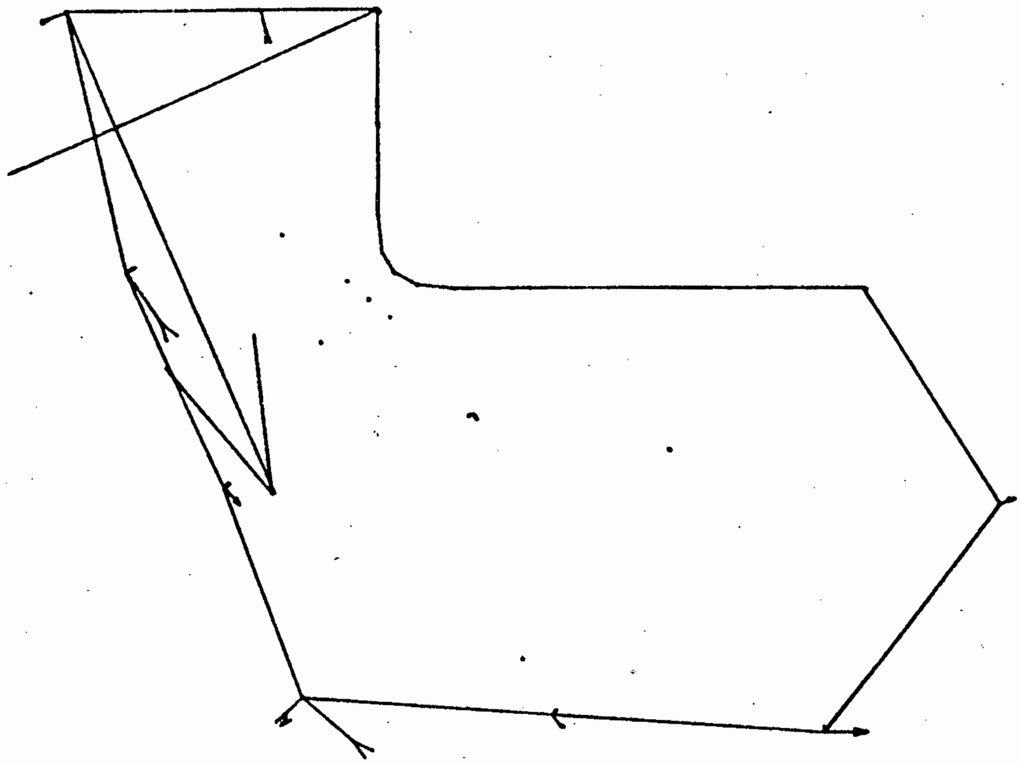

Figure F1. The Principal Stress Vectors of FEM2C1. The ill-conditioning effects apparent at the left-hand side of the mesh of can be attributed to the failure to specify loading elements in the region. The corner nodes are the worst affected.

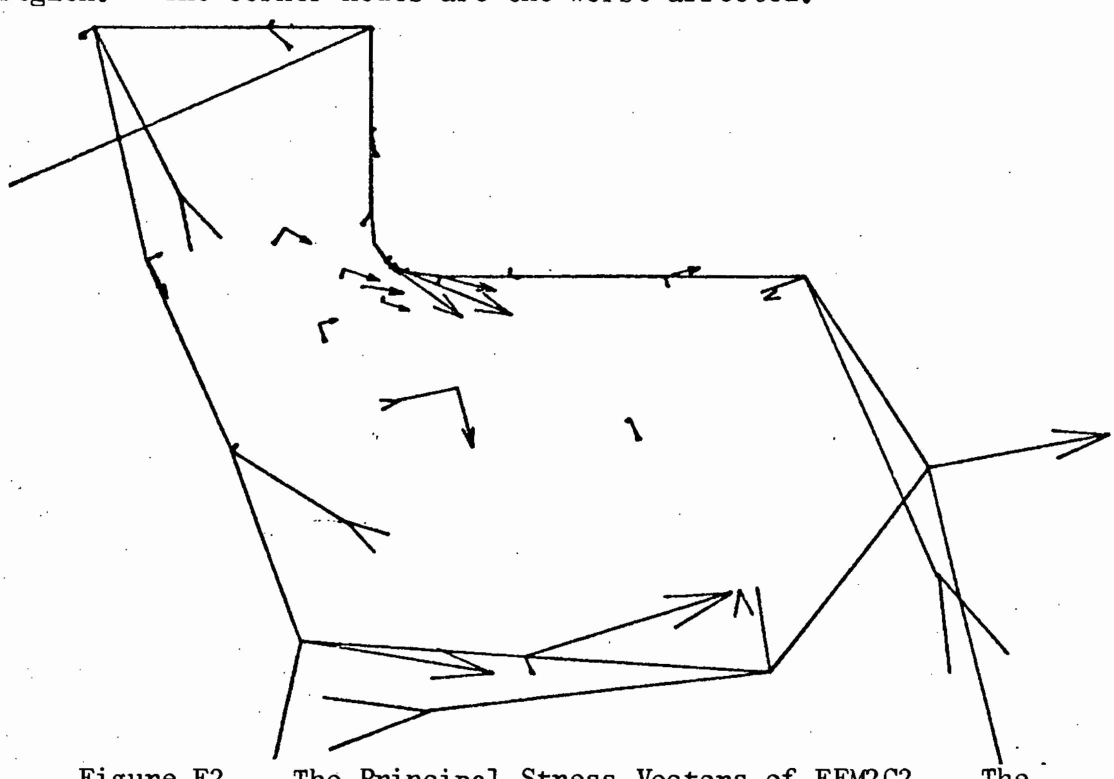

Figure F2. The Principal Stress Vectors of FEM2C2. The effects of ill-conditioning are relatively minor compared with those of the other runs of the series. The fact that this run did not produce perfect results can be attributed to the failure to match exactly the strain-displacement equations with the force-displacement equations to be replaced.

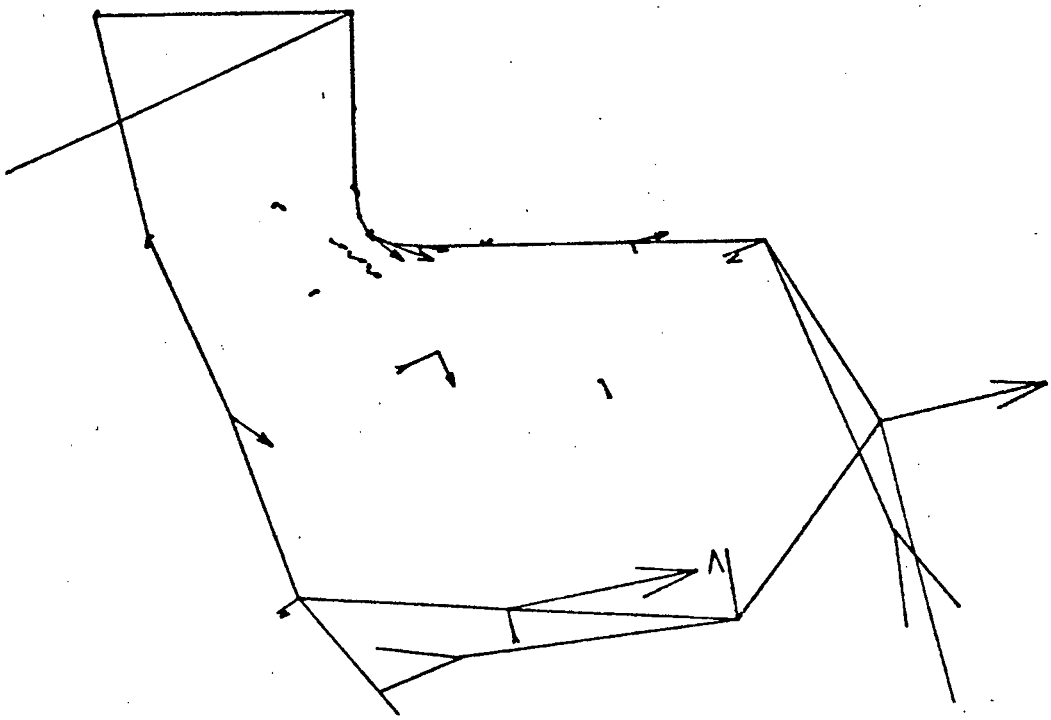

Figure F3. The Principal Stress Vectors of FEM2C3. The ill-conditioned results may be attributed to the over-contraining of the mesh as well as the failure to specify loading elements in the bottom left-hand corner of the mesh.

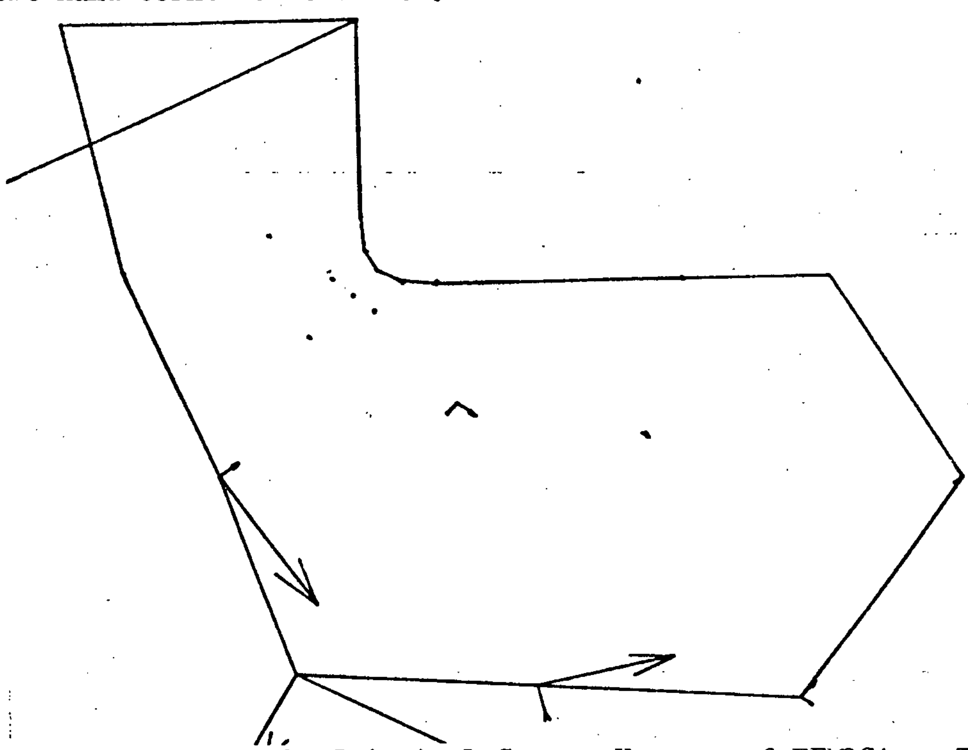

Figure F4. The Principal Stress Vectors of FEM2C4. This run was made to test the effect of specifying as free a corner node in a region of the mesh not assosciated with loading elements. The above plot demonstrates the resulting effects of ill-conditioning.

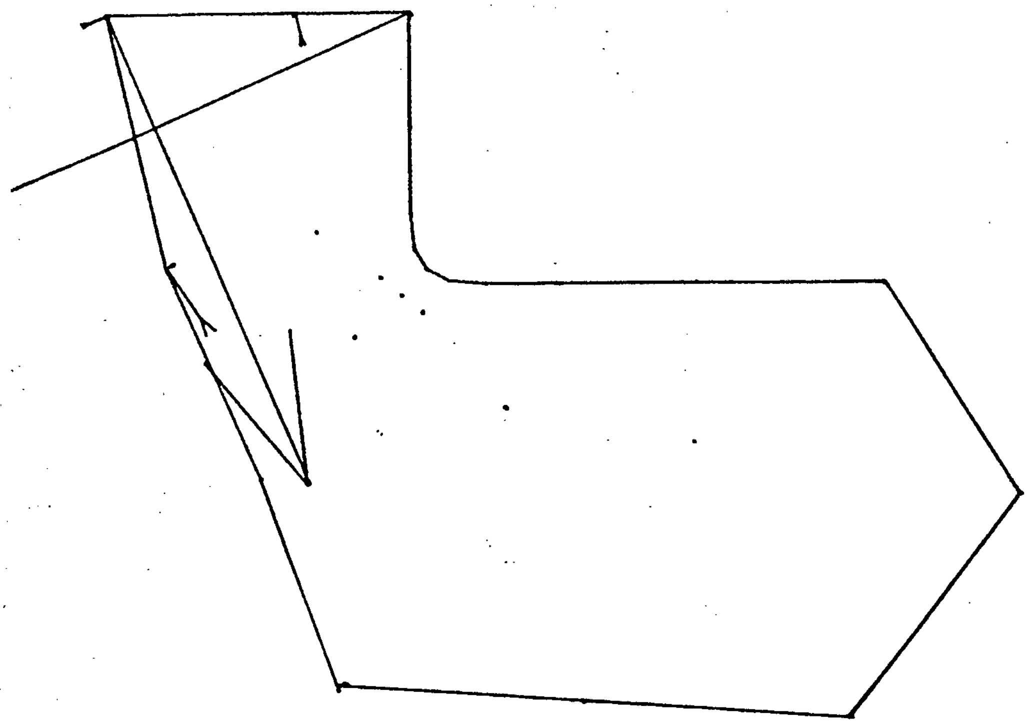

Figure F5. The Principal Stress Vectors of FEM2C6. The effects of ill-conditioning are more apparent in this run than they are in run FEM2C1.

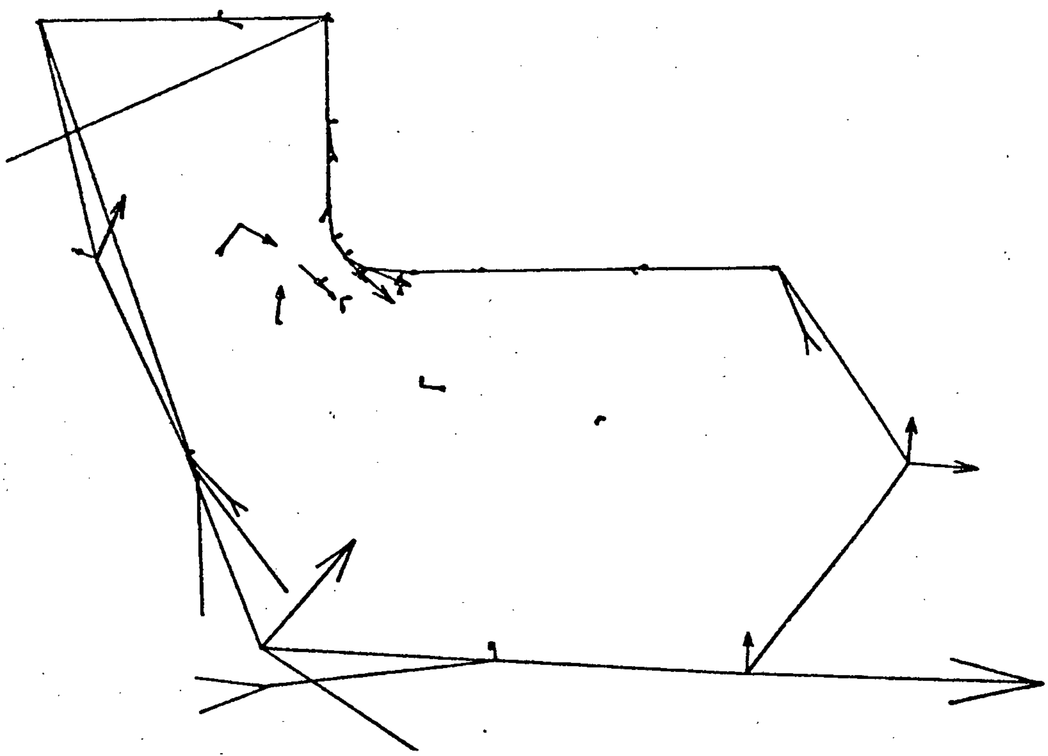

Figure F6. The Principal Stress Vectors of FEM2C7. The effects of ill-conditioning are more apparent in this run than they are in run FEM2C2, as evidenced by the deterioration in the stresses in region of the fillet.

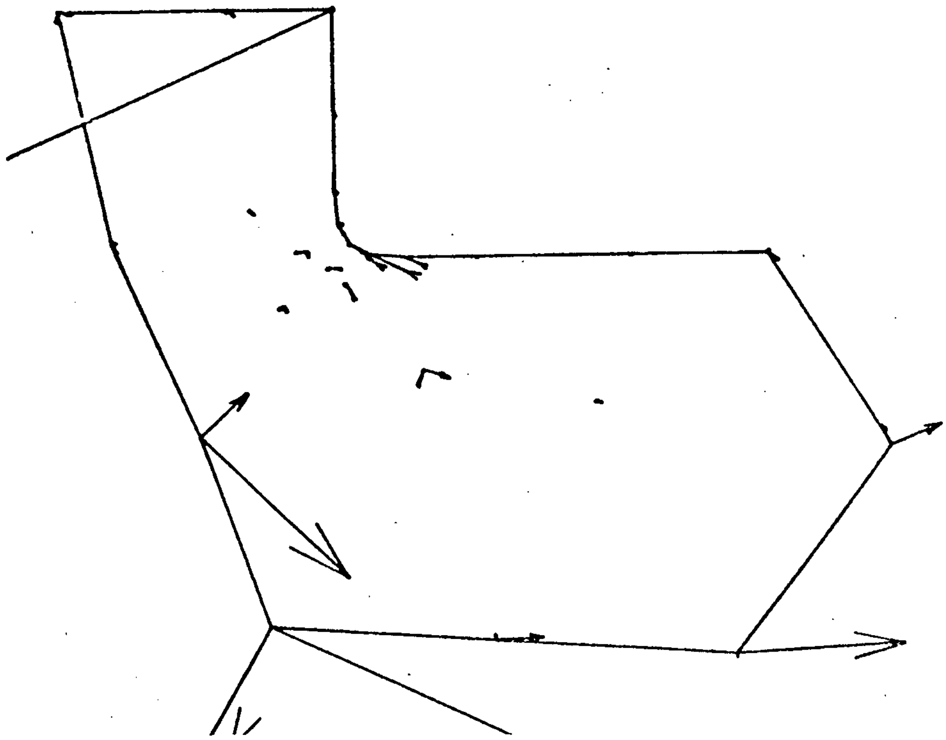

Figure F7. The Principal Stress Vectors of FEM2C8. Comparing the above results with those of run FEM2C7, it is demonstrated how the absence of the two strain-displacement equations from element 30 (which occurs in FEM2C8) results in severe ill-conditioning, as evidenced by the compressive stresses in the region of the fillet.

APPENDIX G

THE PHASE TWO TESTING OF MODEL FEM3

This appendix is related to sections 4.336 and 4.344 of the report. The reader is referred to Appendix C for illustrations of the mesh.

The characteristics of the runs made in the series are listed in table G1.

RUN	DISPLACEMENT BOUNDARY CONDITIONS		LOADING
	fixed nodes	indeterminate nodes	elements
FEM31	axes of symmetry	none	none (RHS forces)
FEM32	ditto	92x,93x,95x, 102x,103x	7,29
FEM33	bottom axis symm.,1y	LHS and RHS	7,19,29
FEM34	ditto	ditto	4,29,33
FEM35	1xy,92y	axes of symmetry	7,19,29,33,36,37
FEM36	ditto	all internal boundaries	7,19,29,33,36, 37,39,40
FEM37	1xy,3x	ditto	ditto
FEM38	LHS axis,1x	bottom axis symm.,RHS	7,19,29,33,37,39,40
FEM39	none	all internal boundaries	1,8,13,16,26, 29,36,39,40

Table G1. The Characteristics of the Runs. The terms LHS and RHS are abbreviations of left- and right-hand sides respectively.

Copies of the results taken from the graphics programme STRESSPLOT are presented in the following pages of this appendix.

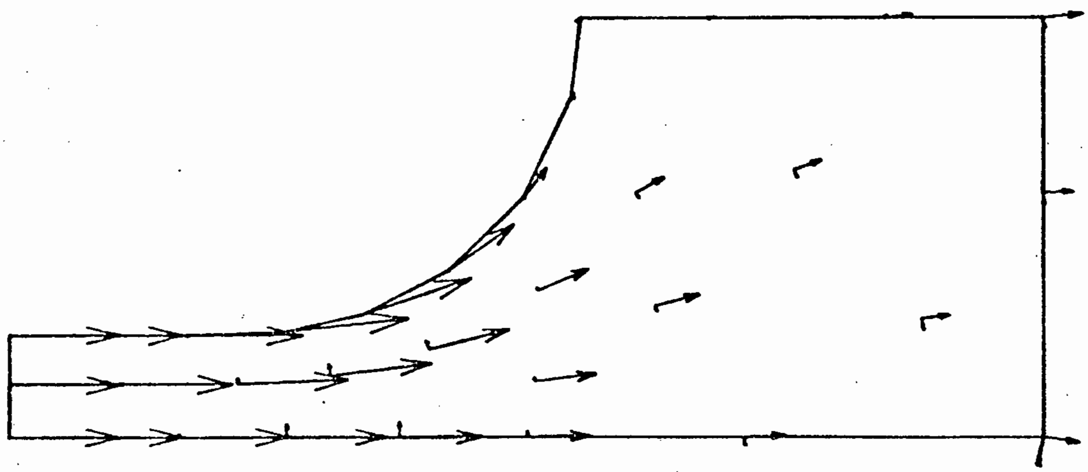

Figure G1. The Principal Stress Vectors of FEM31. The quality of the above plot clearly demonstrates the ability of the programme to accurately solve conventional cases of finite element analysis.

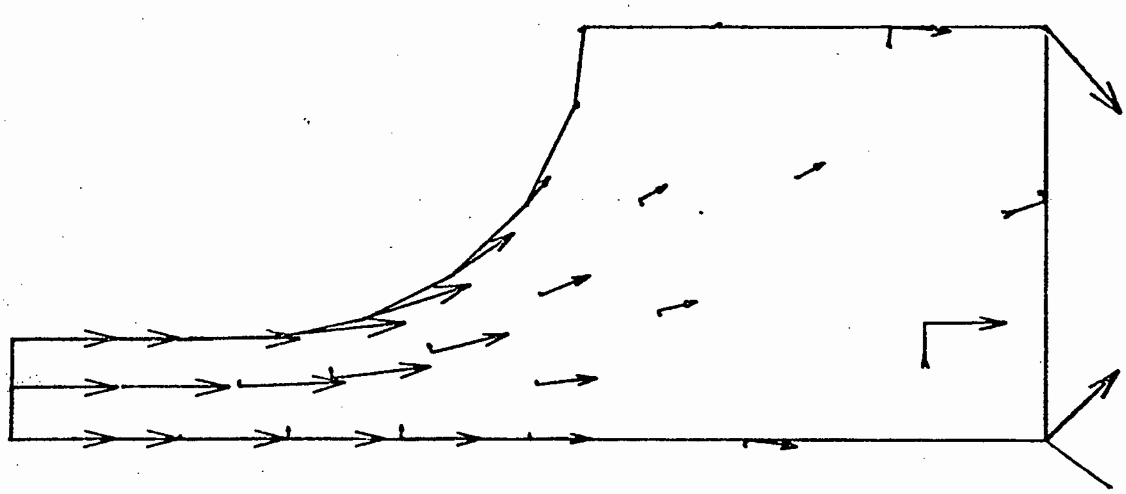

Figure G2. The Principal Stress Vectors of FEM32. This plot compares favourably to that of FEM31, the only variance being in the right-hand side of the mesh, ie. in the vicinity of the indeterminate nodes.

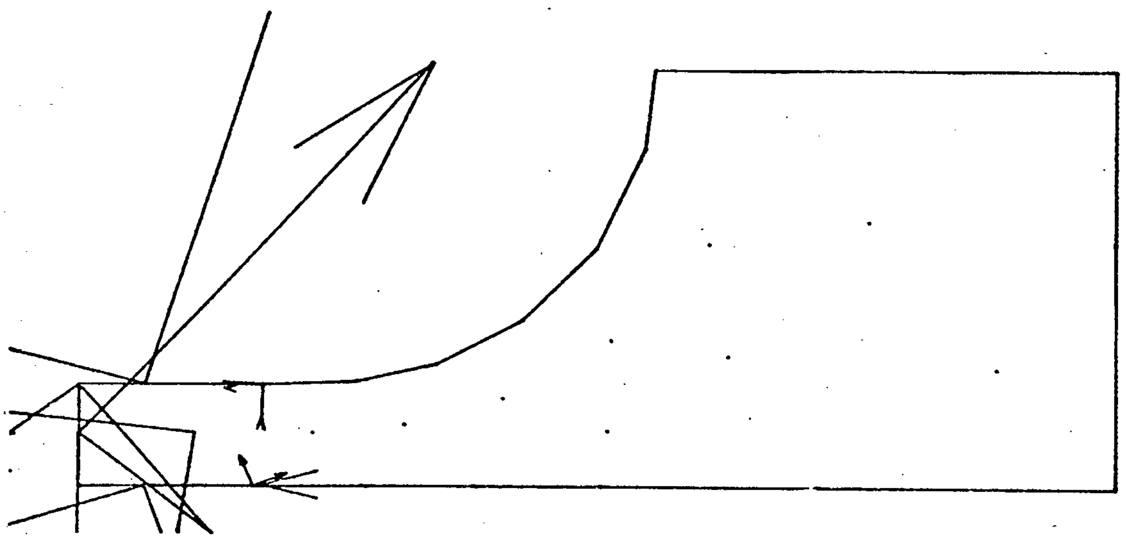

Figure G3. The Principal Stress Vectors of FEM33. The ill-conditioning effects located at the left-hand side of the mesh can be attributed to the failure to specify loading elements from the immediate vicinity.

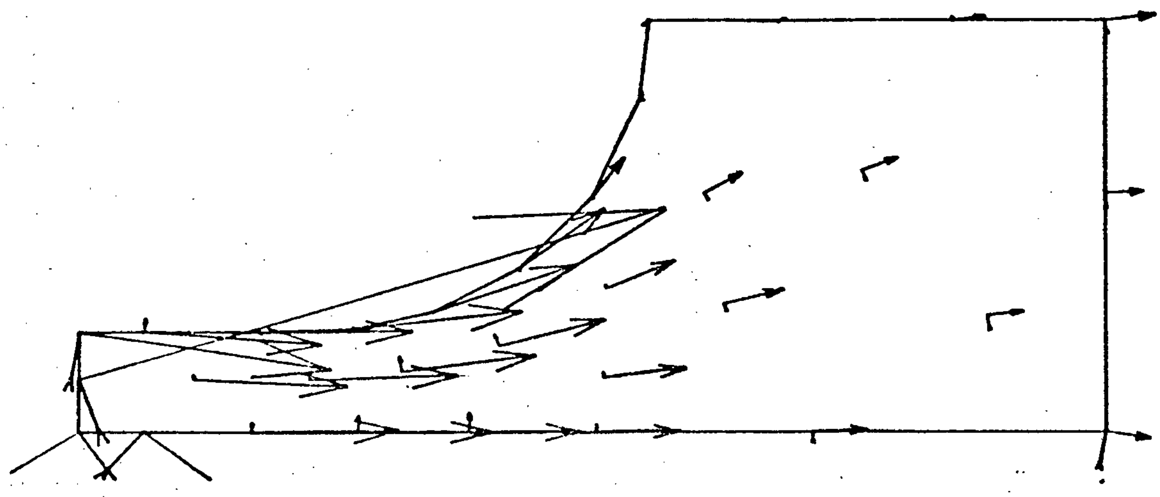

Figure G4. The Principal Stress Vectors of FEM34. The above plot demonstrates the reduction in the effect of ill-conditioning (cf. figure G3) which results from the specification of a loading element assosciated with the left-hand side of the mesh.

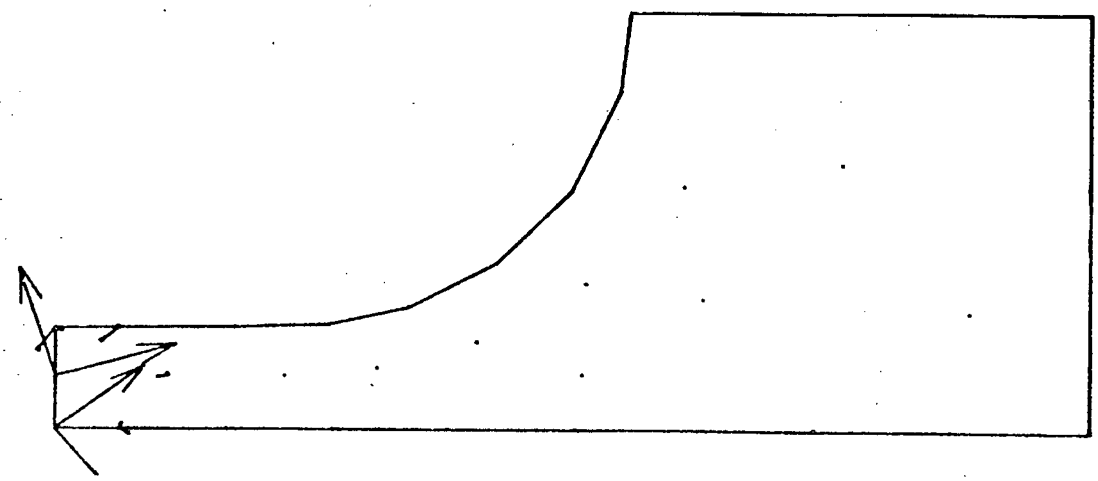

Figure G5. The Principal Stress Vectors of FEM35. The ill-conditioned nodes of the left-hand region are clearly evident.

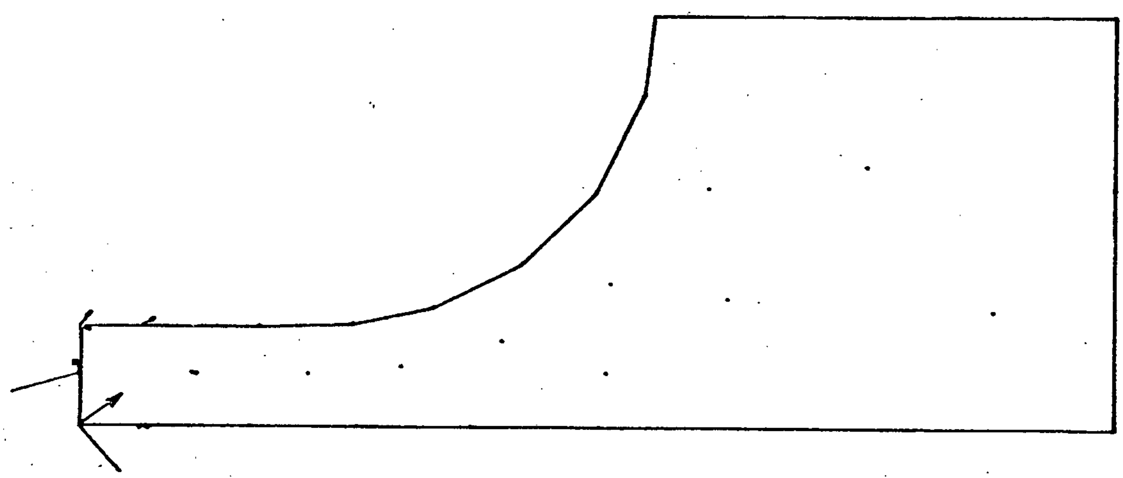

Figure G6. The Principal Stress Vectors of FEM36. The replacement of the force specifications on the right-hand side of the mesh (as for FEM35) by indeterminate specifications and strain loadings can be seen to have little effect on the ill-conditioning of the system.

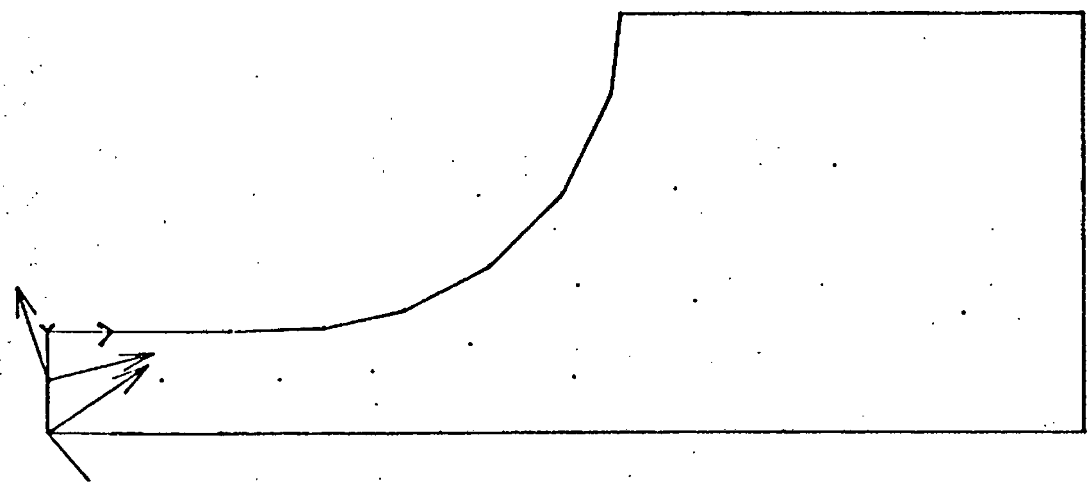

Figure G7. The Principal Stress Vectors of FEM37. The specification of the fixed displacement boundary condition on the left-hand side rather than the right-hand side of the mesh (cf. FEM36) can be seen to have little effect on the ill-conditioning of the system.

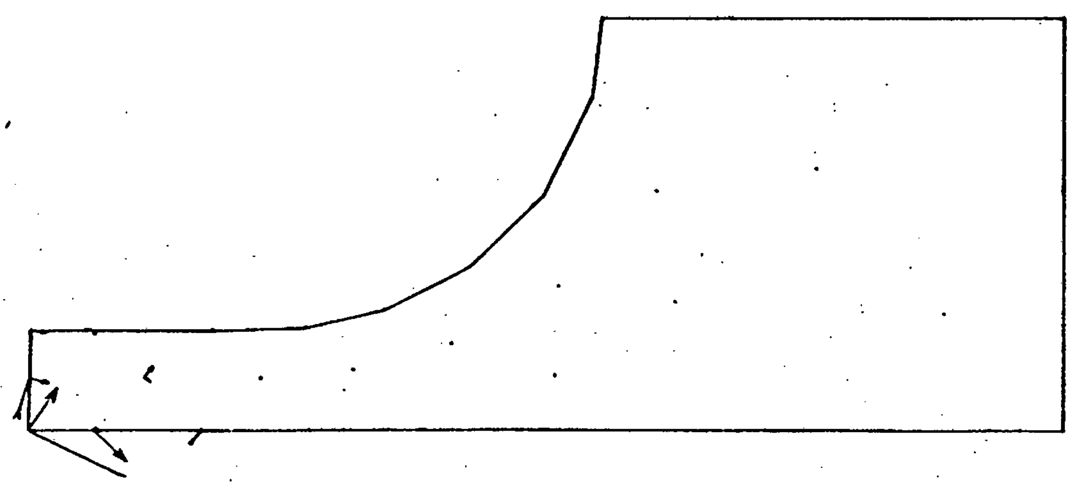

Figure G8. The Principal Stress Vectors of FEM38. The specification of fixed displacement boundary conditions along the left-hand side of the mesh can be seen to result in a decrease of the effects of ill-conditioning in the region.

In tables H2,H3 and H4 the displacements of the vertex nodes, computed in the runs of the series, are expressed as absolute percentage errors of the corresponding displacement values of run FEMST1.

NODES	FEMST2	FEMST3	FEMST4	FEMST5	FEMST6	FEMST7
1x	.000	.000	.000	.023	.000	.004
2x	.000	.016	.002	.079	.002	.002
2y	.000	.034	.000	.011	.000	.006
3x	.000	.000	.000	.031	.003	.003
3y	.000	.308	.009	.074	.080	.083
4x	.000	.003	.003	.012	.003	.000
4y	.000	.066	.000	.389	.029	.029
5x	.000	.000	.000	.011	.006	.000
6x	.000	.000	.000	.009	.000	.000
6y	.000	.139	.014	.551	.104+01	.077
7x	.000	.003	.000	.017	.014	.000
7y	.000	.007	.004	.021	.284	.000

Table H2. Percentage Errors in the Displacements of Runs FEMST2 to FEMST7

NODES	FEMST8	FEMST9	FEMST10	FEMST11	FEMST12	FEMST13
1x	.000	.000	.008	.562+07	.129+03	.000
2x	.002	.033	.002	.909+07	.542+02	.002
2y	.000	.045	.000	.746+07	.051	.000
3x	.000	.003	.007	.125+07	.114+03	.000
3y	.067	.245	.051	.229+09	.335+01	.003
4x	.003	.003	.003	.244+05	.103+03	.003
4y	.015	.015	.007	.556+07	.108+01	.000
5x	.006	.000	.006	.711+04	.191+03	.000
6x	.000	.000	.004	.568+04	.106+06	.000
6y	.697	.098	.146	.461+06	.428+08	.049
7x	.014	.000	.010	.431+05	.103+06	.000
7y	.217	.007	.082	.148+06	.178+09	.000

Table H3. Percentage Errors in the Displacements of Runs FEMST8 to FEMST13

NODES	FEMST14	FEMST15	FEMST16	FEMST17	FEMST18	FEMST19	FEMST20
1x	.019	.074	.113+03	.016	.269+03	.111+02	.357+04
2x	.009	.347	.417+03	.007	.855+03	.123+04	.389+05
2y	.006	.555	.134+03	.129	.212+04	.183+03	.571+03
3x	.017	.065	.387+03	.003	.239+03	.132+04	.113+05
3y	.183	.241+01	.470+05	.183+01	.711+04	.163+06	.187+06
4x	.016	.040	.112+04	.006	.119+03	.278+04	.159+06
4y	.074	.165+01	.628+05	.051	.207+04	.933+05	.123+07
5x	.022	.017	.639+04	.000	.250+03	.665+04	.107+05
6x	.022	.018	.153+11	.004	.177+03	.135+05	.379+05
6y	.105	.200+01	.312+13	.077	.855+05	.475+07	.195+08
7x	.107	.048	.246+12	.010	.121+04	.304+05	.442+06
7y	.014	.060	.813+13	.142	.431+05	.292+07	.726+07

Table H4. Percentage Errors in the Displacements of Runs FEMST14 to FEMST20

APPENDIX J

THE PHASE FOUR TESTING OF THE PHYSICAL DATA MODELS

This appendix is related to section 4.5 of the report. The reader is referred to Appendix C for the illustrations of the meshes.

The characteristics of the two runs made in this phase are listed in table J1.

RUN	DISPLACEMENT BOUNDARY CONDITIONS		LOADING
	fixed nodes	indeterminate nodes	elements
FEM2BR	74y,75xy	70xy,72x,73xy,74x,76xy,77xy,78xy,80xy,82xy,85xy,86xy,89x	25,26,27,29,31,32,34
FEM2CR	71y,72xy	48xy,49xy,54x,55xy,63x,66xy,70xy,71x,73xy,74xy,75xy,77xy,78xy,79xy	14,15,20,25,26,27,28,29,30

Table J1. The Characteristics of the Runs

In table J2, the results of runs FEM2BR and FEM2CR (in terms of the displacements of the vertex nodes of the elements) are compared on a percentage error basis. The formula used can be expressed as

$$\text{percentage error} = \frac{x - y}{x} \times 100$$

where x = nodal displacement in FEM2CR

y = nodal displacement in FEM2BR

The nodes are numbered according to the FEM2C configuration.

NODE	x coords.	y coords.	NODE	x coords.	y coords.
1	.251	.054	38	.939	.047
3	.265	.009	43	.719	.183
6	.355	.059	45	1.382	.142
9	.547	.027	48	2.327	.013
12	.508	.079	54	.294	.063
17	.677	.059	59	.824	.407
19	.587	.081	61	1.947	.368
21	.650	.095	63	.885	4.452
24	.742	.076	70	6.316	.309
30	.688	.105	74	1.713	.216
32	.706	.134	77	2.536	.311
34	.818	.094	79	.646	.065

Table J2. Percentage Variations in the Displacements of Runs FEM2BR and FEM2CR